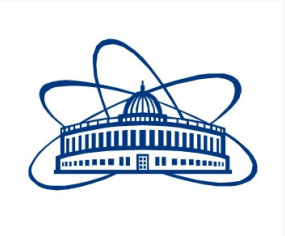
Generation of angular momentum in spontaneous fission of ^{252}Cf

A. Rahmatinejad

T. M. Shneidman, N. V. Ryzhkov, A. V. Andreev, G. G. Adamian, N. V. Antonenko

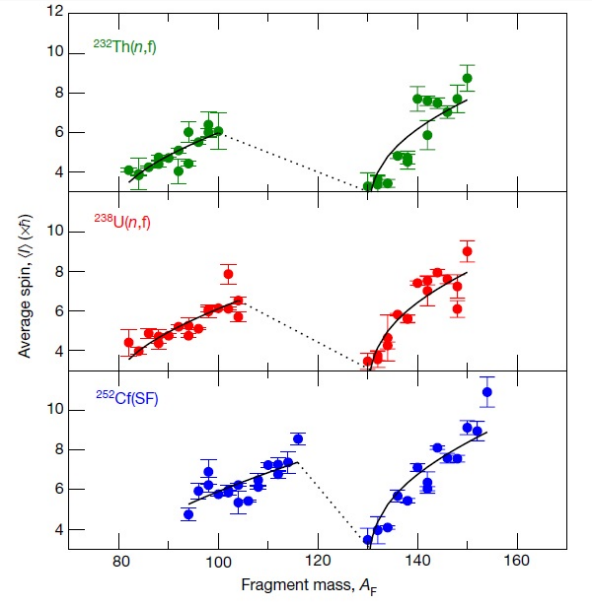
May, 2026

Joint Institute for Nuclear Research



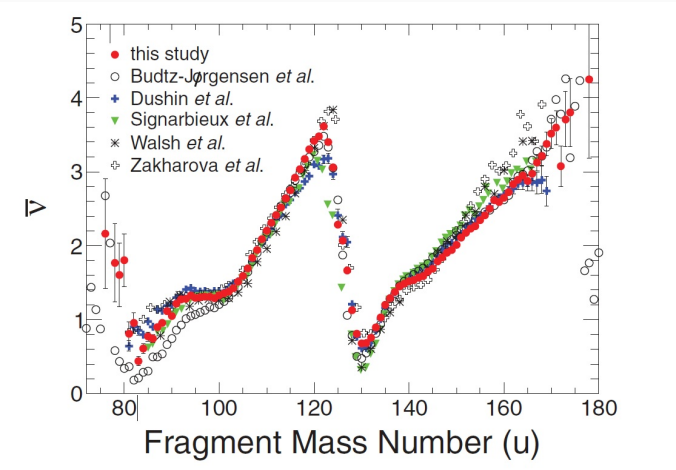
Correlations between fragment spin and fission observables

Saw-tooth behavior of fragments spin vs mass



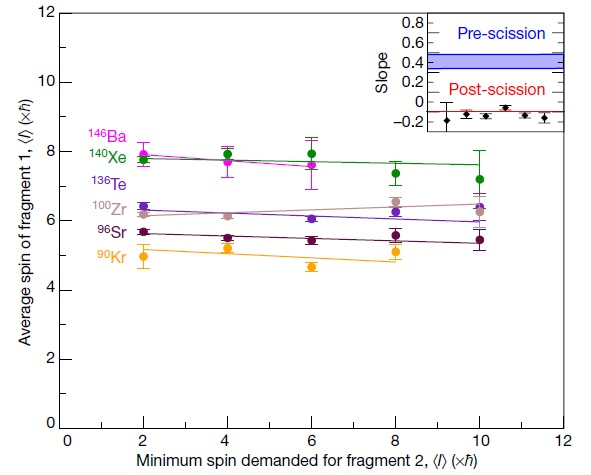
J. N. Wilson et. al, Nature **590**, 566–570 (2021).

Average number of emitted neutrons vs mass



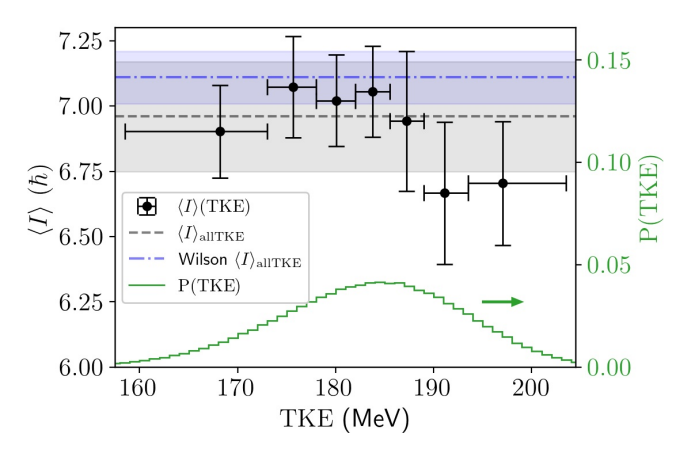
A. Göök et al., Phys. Rev. C **90**, 064611 (2014).

Absence of correlation between fragments spin



J. N. Wilson et. al, Nature **590**, 566–570 (2021).

Weak correlation between spin and total kinetic energy



N. P. Giha *et al.*, Phys. Rev. C, **111** 014603 (2025).

Outline

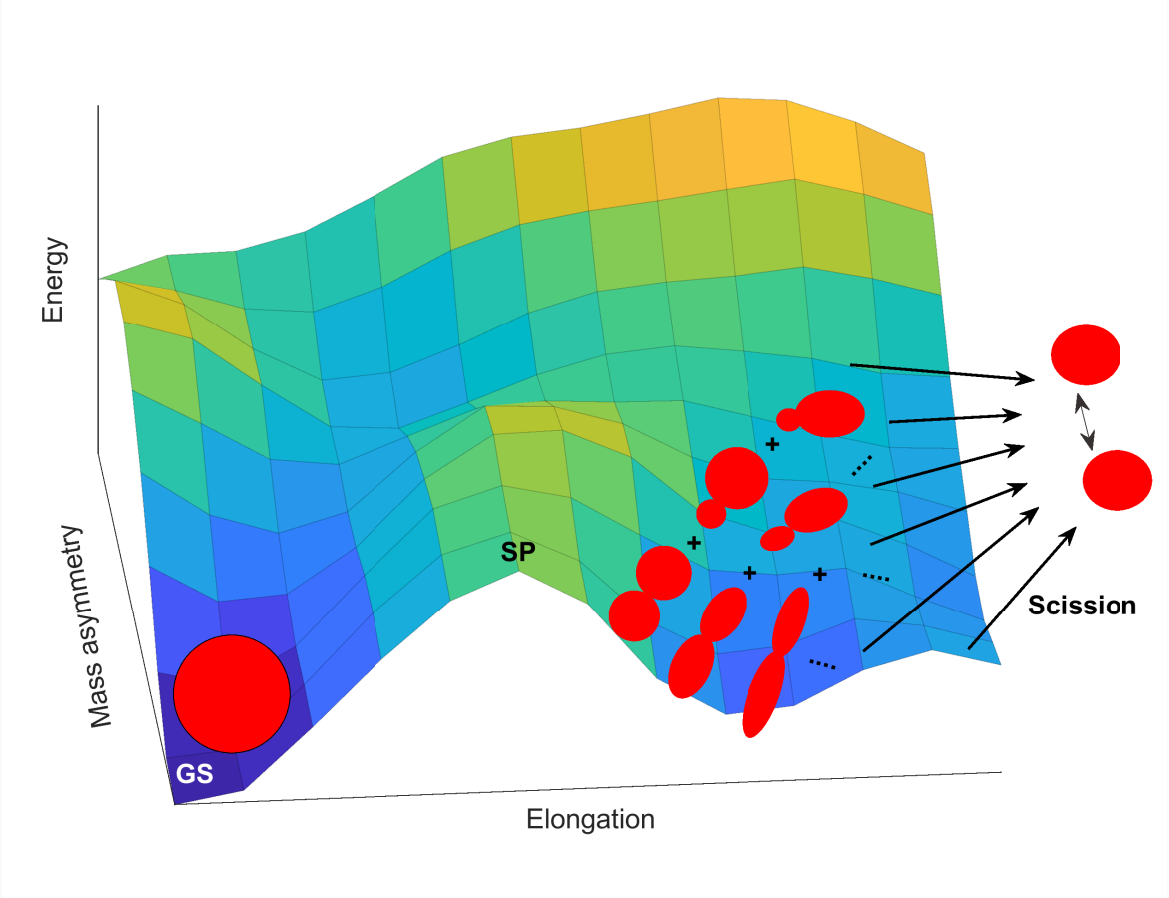
- Overview of the fission model
- Treatment of angular momentum
- Results for spontaneous fission of ^{252}Cf
  - Main observables
  - Correlations between observables
- Summary



Fission model

Fission model

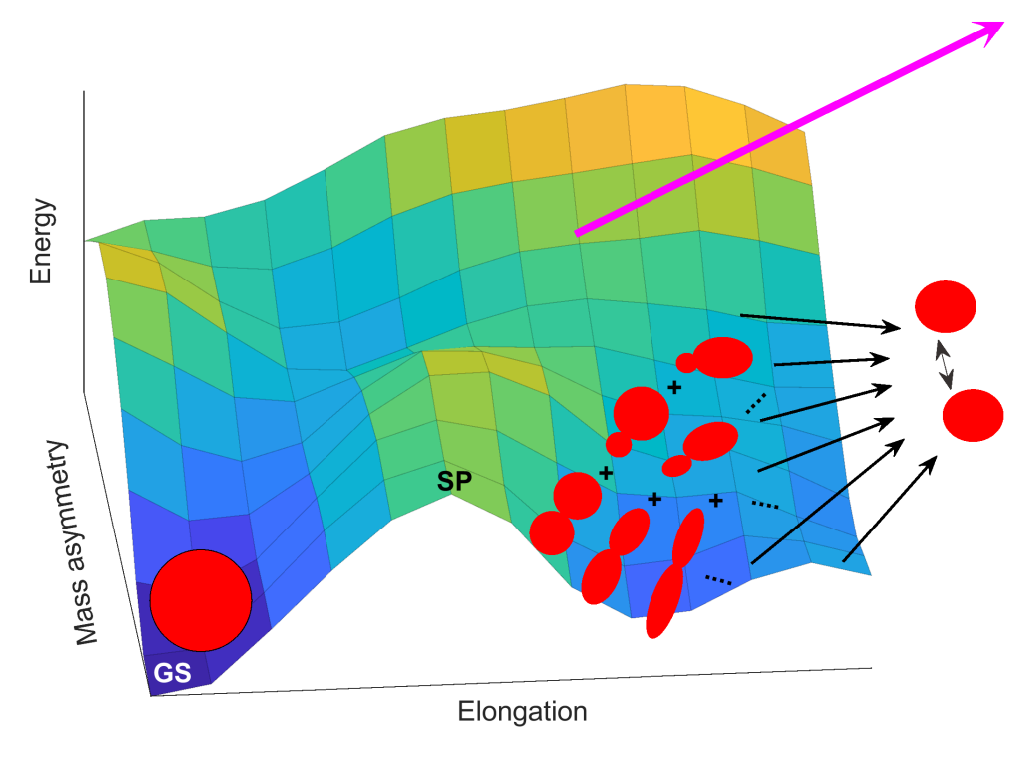
Distribution of primary fission fragments are obtained at scission



$$\frac{\mathrm{d}}{\mathrm{d}t}P(n,t) = \sum_{n'}\left[\Lambda(n'|n)P(n',t) - \Lambda(n|n')P(n,t)\right] - \Lambda_{decay}(n)P(n,t)$$

$$n = (A_i, Z_i, \beta_i, i = 1, 2)$$

Fission model: IJMPE 33 (2024) 2441018/PRC 111 (2025) 0046600/PRC 112 (2025) 044610

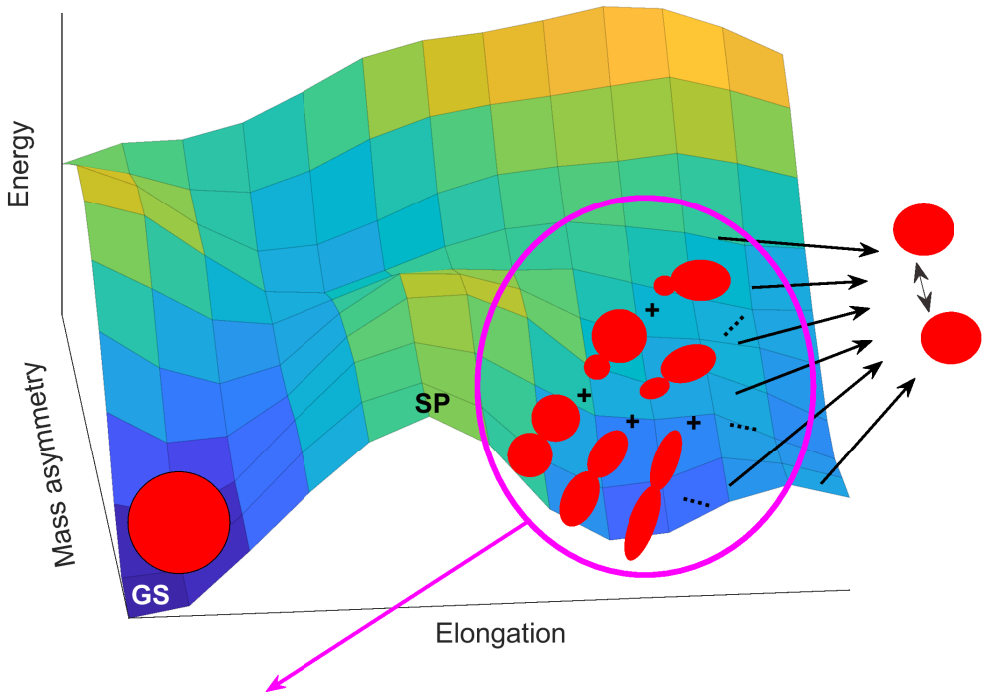


Potential energy surface:

- Mic-mac model
  A. Andrev et al., EPJA 30 (2006) 579.
- Deformation- and excitation energy-dependent shell effects
  AR et al, EPJA 60 (2024) 214.

* The damping of microscopic corrections is included consistently in the PES and level densities.

Fission model: IJMPE 33 (2024) 2441018/PRC 111 (2025) 0046600/PRC 112 (2025) 044610



Potential energy surface:

- Mic-mac model
  A. Andreev et al., EPJA 30 (2006) 579.
- Deformation- and excitation energy-dependent shell effects
  AR et al, EPJA 60 (2024) 214.

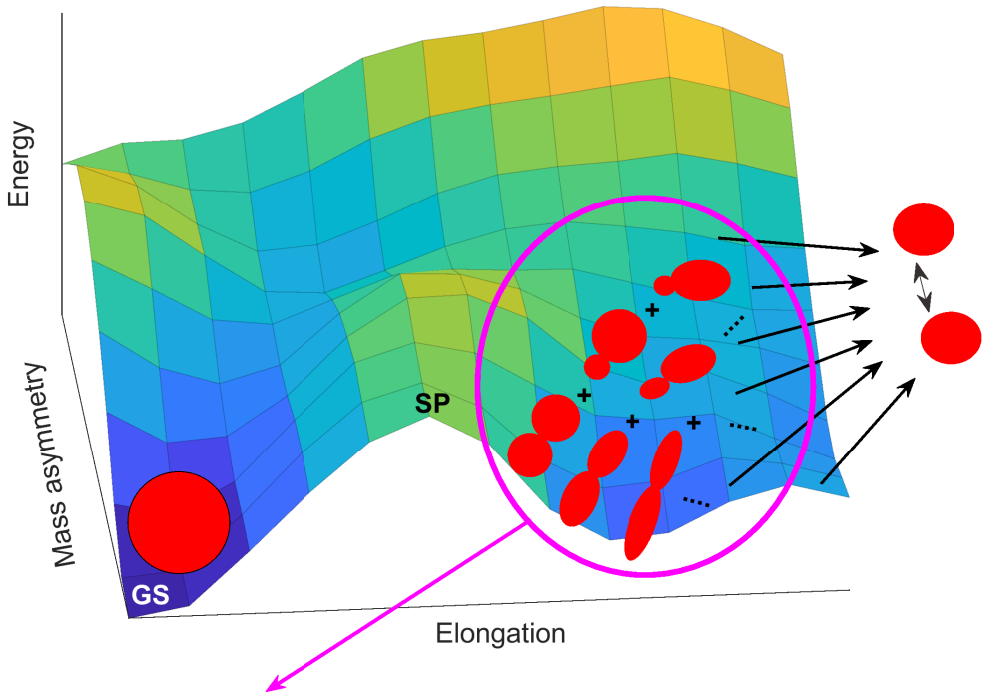
Transition rates and yields:

- Nuclear level densities:
  $\rho_{int}(E^*, n) =$
  $\int \rho_1(A_1, Z_1, \beta_1, \varepsilon)\rho_2(A_2, Z_2, \beta_2, E^* - \varepsilon)\mathrm{d}\varepsilon.$

  Excitation energy, deformation and shell effects.

  A. N. Bezbakh et al., EPJA 50 (2014) 97.
  AR et al., PRC 103 (2021) 034309.
  AR et al., PRC 105 (2022) 044328.

Fission model: IJMPE 33 (2024) 2441018/PRC 111 (2025) 0046600/PRC 112 (2025) 044610



Potential energy surface:

- Mic-mac model
  A. Andrev et al., EPJA 30 (2006) 579.
- Deformation- and excitation energy-dependent shell effects
  AR et al, EPJA 60 (2024) 214.

Collective effects:

- $\rho(E^*, n) = \sum_x \rho_{int}(E^* - E_x^n, n)$.
  AR et al., PRC 101 (2020) 054315.

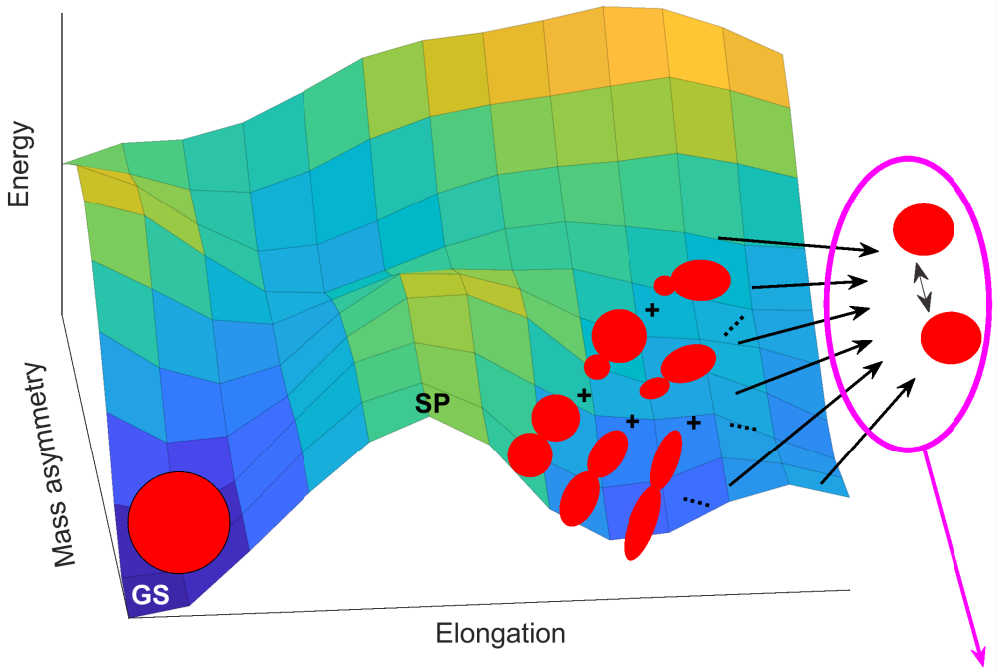
Transition rates and yields:

- Nuclear level densities:
  $\rho_{int}(E^*, n) =$
  $\int \rho_1(A_1, Z_1, \beta_1, \varepsilon)\rho_2(A_2, Z_2, \beta_2, E^* - \varepsilon)\mathrm{d}\varepsilon.$

  Excitation energy, deformation and shell effects.

  A. N. Bezbakh et al., EPJA 50 (2014) 97.
  AR et al., PRC 103 (2021) 034309.
  AR et al., PRC 105 (2022) 044328.

Fission model: IJMPE 33 (2024) 2441018/PRC 111 (2025) 0046600/PRC 112 (2025) 044610



Potential energy surface:

- Mic-mac model
  A. Andrev et al., EPJA 30 (2006) 579.
- Deformation- and excitation energy-dependent shell effects
  AR et al, EPJA 60 (2024) 214.

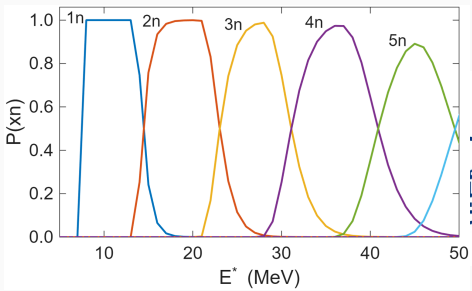
Collective effects:

- $\rho(E^*, n) = \sum_x \rho_{int}(E^* - E_x^n, n)$.
  AR et al., PRC 101 (2020) 054315.

Neutron emission probabilities:

- Monte-Carlo simulation

  AR et al., PEPAN Lett. 19 (2022) 470.
  AR et al., PLB 844 (2023) 138099.



Transition rates and yields:

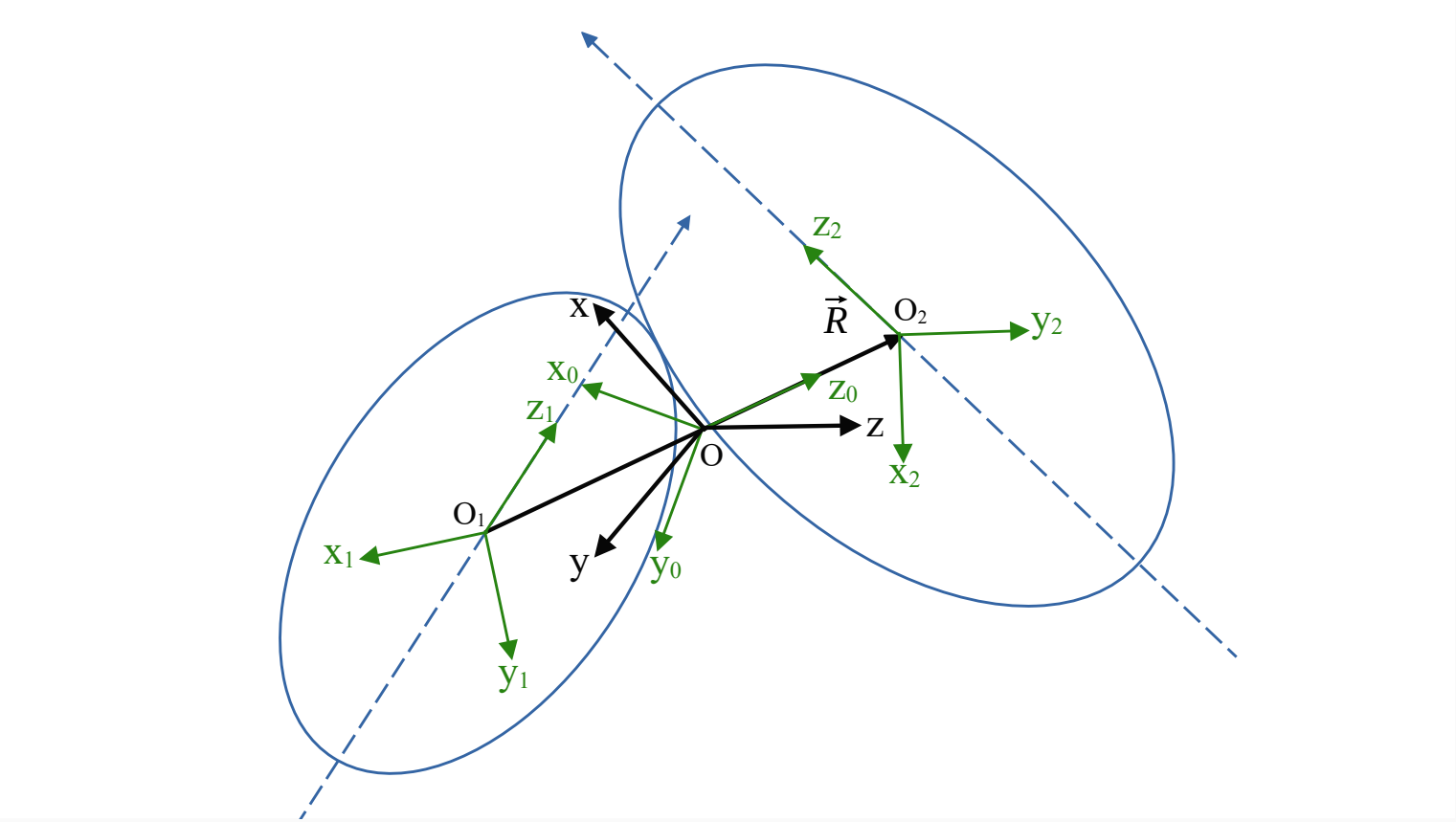
- Nuclear level densities:
  $\rho_{int}(E^*, n) =$
  $\int \rho_1(A_1, Z_1, \beta_1, \varepsilon)\rho_2(A_2, Z_2, \beta_2, E^* - \varepsilon)\mathrm{d}\varepsilon.$

  Excitation energy, deformation and shell effects.

  A. N. Bezbakh et al., EPJA 50 (2014) 97.
  AR et al., PRC 103 (2021) 034309.
  AR et al., PRC 105 (2022) 044328.

Angular momentum distribution

Angular motion at scission PRC 111 (2025) 0046600/PRC 112 (2025) 044610



$\Omega_{1,2} = (\phi_{1,2}, \theta_{1,2}, 0)$ – orientation of fragments with respect to the lab. system

$\tilde{\Omega}_{1,2} = (\varepsilon_{1,2}, \gamma_{1,2}, 0)$ – orientation of fragments with respect to the body-fixed system

R$= (R, \theta_R, \phi_R)$ – vector connecting centers of the fragments.

Angular vibrations at scission

Kinetic energy ($\mathbf{I_0} + \mathbf{I_1} + \mathbf{I_2} = \mathbf{0}$):

$$T = \frac{\hbar^2(\hat{I}_1 + \hat{I}_2)^2}{2\mu R_m^2} + \frac{\hbar^2 \hat{I}_1^2}{2\Im_1} + \frac{\hbar^2 \hat{I}_2^2}{2\Im_2} = \frac{\hbar^2 \hat{I}_1^2}{2\Im_{b,1}} + \frac{\hbar^2 \hat{I}_2^2}{2\Im_{b,2}} + \frac{\hbar^2 \hat{I}_1 \hat{I}_2}{\mu R_m^2};$$

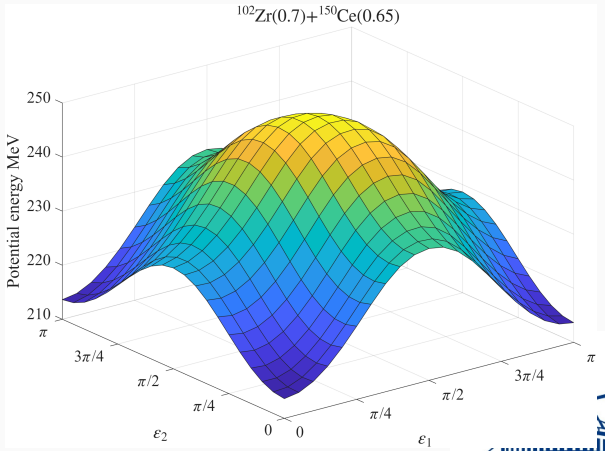
$$\Im_{bi} = \frac{\Im_i \mu R_m^2}{\Im_i + \mu R_m^2} \ll \mu R_m^2$$

For large enough deformations ($\beta_i \geqslant 0.15$) Potential energy:

$$V(\tilde{\Omega}_1, \tilde{\Omega}_2) \approx \frac{C_1}{2} \sin^2 \varepsilon_1 + \frac{C_2}{2} \sin^2 \varepsilon_2 + C_{12} \sin^2 \varepsilon_1 \sin^2 \varepsilon_2 \cos(\gamma_1 - \gamma_2)$$

$$V(\varepsilon_1', \varepsilon_2') \approx \frac{C_1}{2} {\varepsilon_1'}^2 + \frac{C_2}{2} {\varepsilon_2'}^2$$

$$(\varepsilon_i' = \varepsilon_i, \pi - \varepsilon_i)$$



Angular vibrations at scission: vibrations of two independent oscillators

Hamiltonian:

$$\hat{H} = \hat{H}_1 + \hat{H}_2 + \hat{H}_{coupl}$$

$$\hat{H}_i = -\frac{\hbar^2}{2}\left[\frac{1}{\varepsilon'_i}\frac{\partial}{\partial\varepsilon'_i}\varepsilon'_i\frac{\partial}{\partial\varepsilon'_i} + \frac{1}{\varepsilon'^2_i}\frac{\partial^2}{\partial\gamma_i^2}\right] + \frac{C_i}{2}\varepsilon'^2_i, \quad (i = 1, 2)$$

$$\hat{H}_{coupl} = \frac{\hbar^2\hat{\mathbf{I}}_1\hat{\mathbf{I}}_2}{\mu R_m^2} + C_{12}\varepsilon'^2_1\varepsilon'^2_2\cos(\gamma_1 - \gamma_2)$$

The eigenstates and eigenvalues of Hamiltonians $\hat{H}_{1,2}$

$$E_{n_iK_i} = \hbar\omega_i(2n_i + |K_i| + 1)$$

$$\phi_{n_iK_i}(\varepsilon'_i, \gamma_i) = N_{n_iK_i}\left(\frac{\varepsilon'^{K_i}_i}{\varepsilon_{0i}^{K_i+1}}\right)\exp\left(-\frac{\varepsilon'^2_i}{2\varepsilon^2_{0i}}\right)L_{n_i}^{(|K_i|)}\left(\frac{\varepsilon'^2_i}{\varepsilon^2_{0i}}\right)\exp\left(-iK_i\gamma_i\right)$$

$$\omega_i = (C_i/\Im_{bi})^{1/2}, \qquad \varepsilon^2_{0i} = \hbar/(C_i\Im_{bi})$$

Expansion in terms of spherical harmonics

$$\Phi_{n_iK_i}(\varepsilon_i, \gamma_i) = \sum_{I_i} a_{n_iK_i}(I)\,Y_{I_i,K_i}(\varepsilon_i, \gamma_i)$$



J. O. Rasmussen, W. Nörenberg, H. J. Mang, Nucl. Phys. A **136**, 465 (1969).

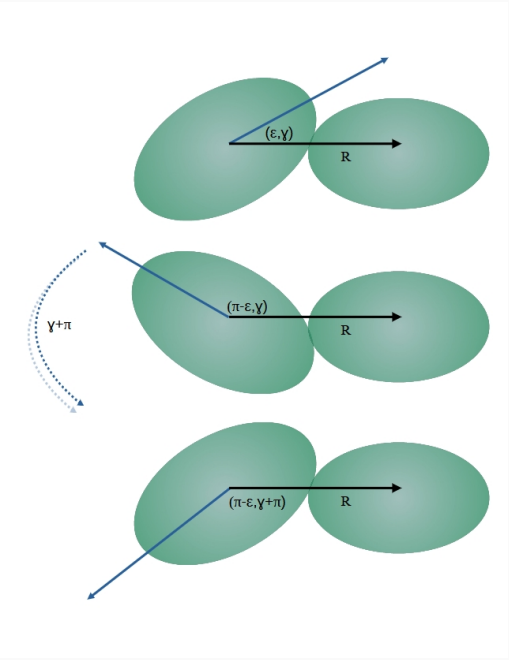
Symmetries

- $\Phi_{n_i K_i}(\varepsilon_i, \gamma_i) \propto exp(-iK_i\gamma_i) \rightarrow \quad K_1 = -K_2 = K$

- $(\varepsilon_i, \gamma_i) \longrightarrow (\pi - \varepsilon_i, \gamma_i + \pi)$

  Symmetrized solution:

$$\Phi^{\pm}_{n_i K_i}(\varepsilon_i, \gamma_i) \sim \phi_{n_i K_i}(\varepsilon_i, \gamma_i) \pm \phi_{n_i K_i}(\pi - \varepsilon_i, \gamma_i + \pi)$$



- $Y_{l_i K_i}(\pi - \varepsilon_i, \gamma_i + \pi) = (-1)^{l_i} Y_{l_i K_i}(\varepsilon_i, \gamma_i)$

$$\Phi^{+}_{n_i K_i}(\varepsilon_i, \gamma_i) = \sum_{\text{even } l_i} a_{n_i l_i K_i} Y_{l_i, |K_i|}(\varepsilon_i, \gamma_i),$$

$$\Phi^{-}_{n_i K_i}(\varepsilon_i, \gamma_i) = \sum_{\text{odd } l_i} a_{n_i l_i K_i} Y_{l_i, |K_i|}(\varepsilon_i, \gamma_i).$$

$\phi^{-}_{n_i K_i}$ is absent for the case of quadrupole deformed fragments.



Total wave function

$$\Psi_{n_1,K_1,n_2,K_2} = \sum_{even l_1,l_2} a^{(1)}_{n_1K_1} a^{(2)}_{n_2K_2} Y_{l_1,K_1}(\varepsilon_1,\gamma_1) Y_{l_2,K_2}(\varepsilon_2,\gamma_2)$$

$$E_{n_1,n_2,K} = \hbar\omega_1(2n_1 + K + 1) + \hbar\omega_2(2n_2 + K + 1)$$

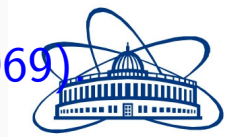
Probabilities of various angular momenta of fragments are independent on each other.

For example, for ground-state $n_1 = n_2 = K_1 = K_2 = 0$:

$$|a^{(i)}(I)|^2 = 2\varepsilon_{0i}^2(2I+1)\exp\left\{-(I+\frac{1}{2})^2\varepsilon_{0i}^2\right\}$$

$$\omega_i = (C_i/\Im_{bi})^{1/2}, \qquad \varepsilon_{0i}^2 = \hbar/(C_i\Im_{bi})$$

J. O. Rasmussen, W. Nörenberg, H. J. Mang, Nucl. Phys. A **136**, 465 (1969)



Stiffness parameters

$$C_i = 2\left[V(R_{pole-neck}, \varepsilon_i = \frac{\pi}{2}) - V(R_{pole-pole}, \varepsilon_i = 0)\right]$$

$$C_i = C_i^{Coul} + C_i^{N}$$

Coulomb part:

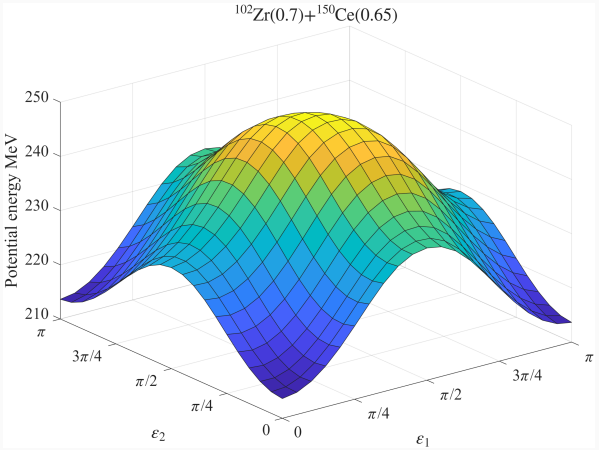
$$V_C = \frac{e^2 Z_1 Z_2}{R_m(\varepsilon_1, \varepsilon_2)} + \sum_{i=1,2} \sqrt{\frac{9}{20\pi}} \frac{e^2 Z_1 Z_2}{R_m^3(\varepsilon_1, \varepsilon_2)} R_i^2 \beta_i P_2(\cos \varepsilon_i)$$

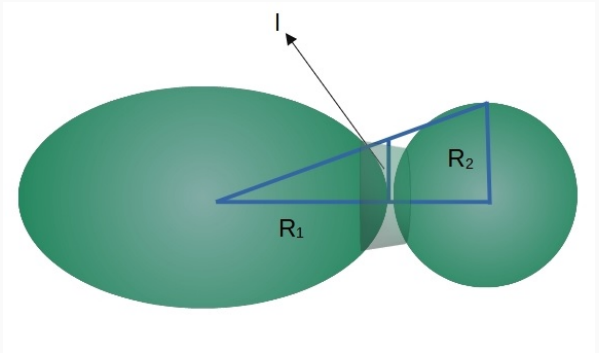
Nuclear part:

$$V_{\text{overlap}} \sim \pi l^2 \Delta z$$

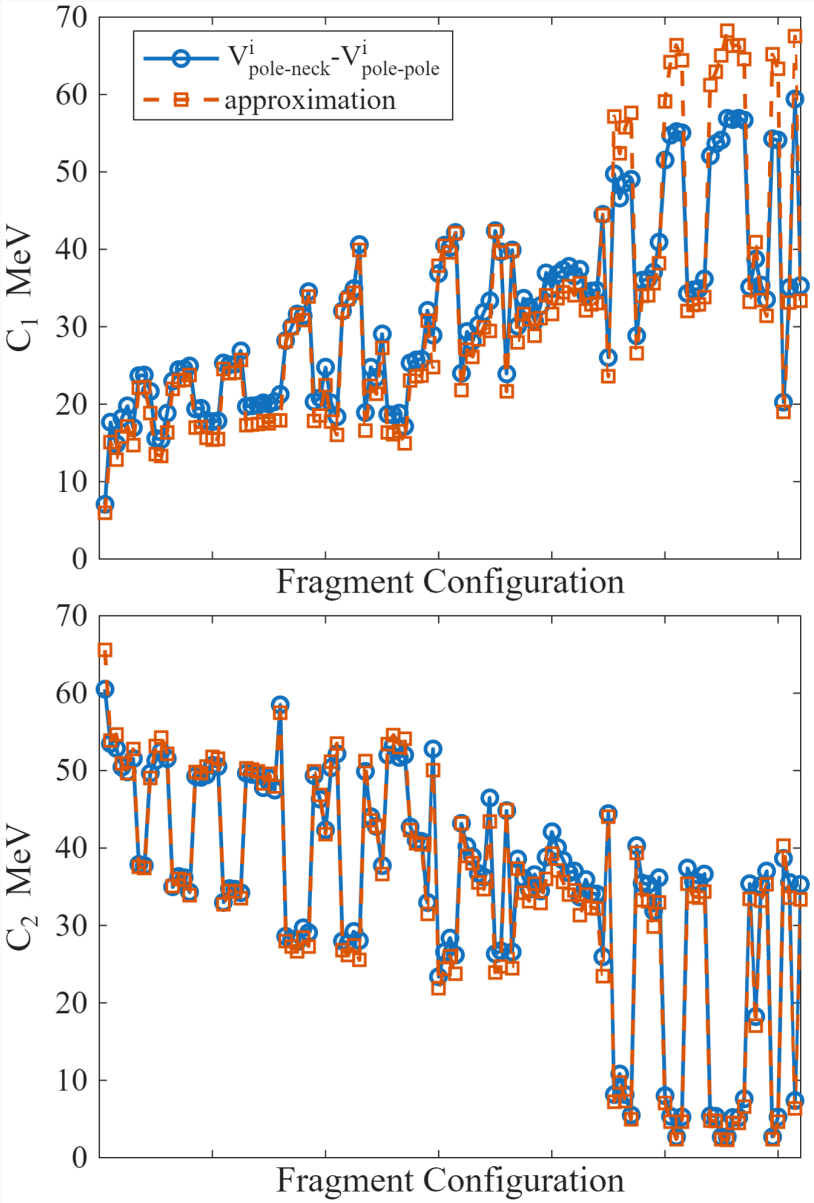
$$l \approx \frac{R_1 R_2}{R_1 + R_2}$$

$$C_i^N = -\alpha \left(\frac{R_{0,i} R_{0,j \neq i}}{R_{0,i} + R_{0,j \neq i}} \right)^2 \beta_i$$





Stiffness parameters: DNS fragments of ^{252}Cf

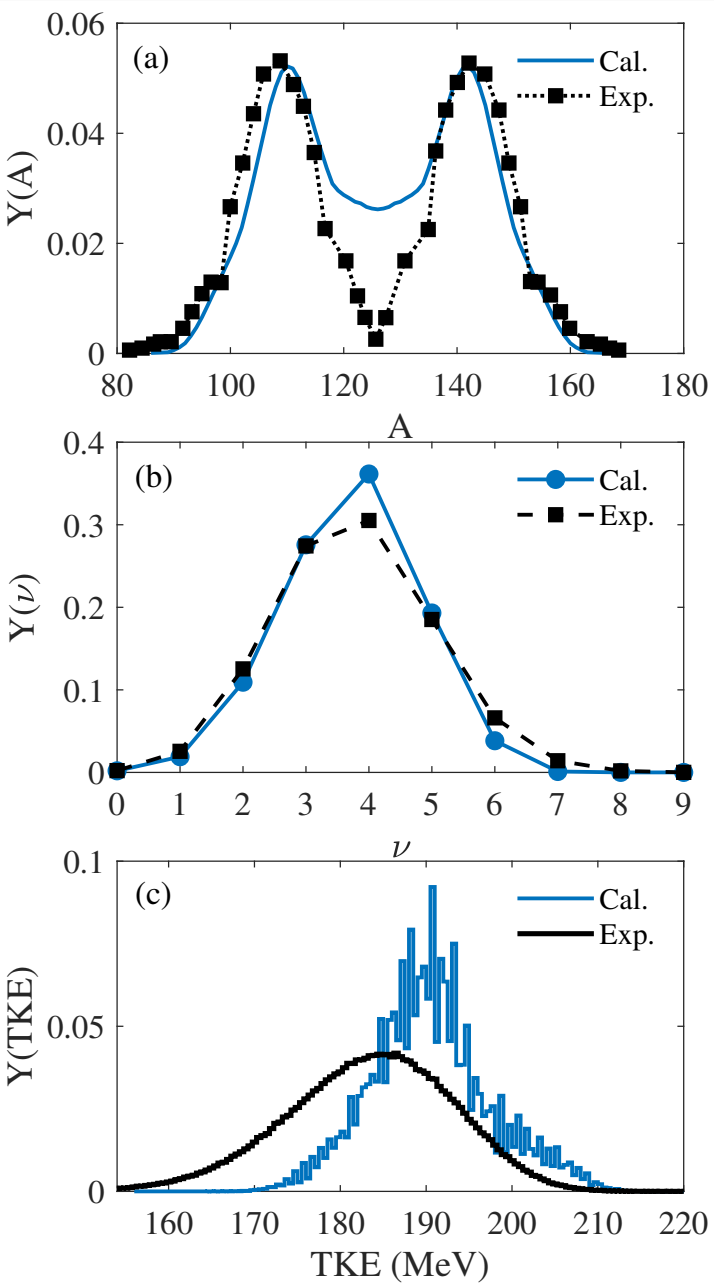


For ^{252}Cf, α is determined by fitting to a set of representative DNS configurations.

$$\alpha = -2.5\mathrm{MeV}$$

Spontaneous fission of ^{252}Cf

Main fission observables



Quantities	Expt.	Cal.
$\langle TKE \rangle$ (MeV)	189 ± 1 [1] 186.8 [2]	189.93
σ_{TKE} (MeV)	9.43 [1] 11.17 [2]	7.36
$\langle A_H \rangle$	145.7 ± 0.1 [1] 143.4 [2]	140.41
$\langle A_L \rangle$	106.3 ± 0.1 [1] 108.6 [2]	111.59
$\langle \nu \rangle$	3.757 ± 0.01 [3] 3.756 ± 0.031 [4]	3.713

Expt. data from:

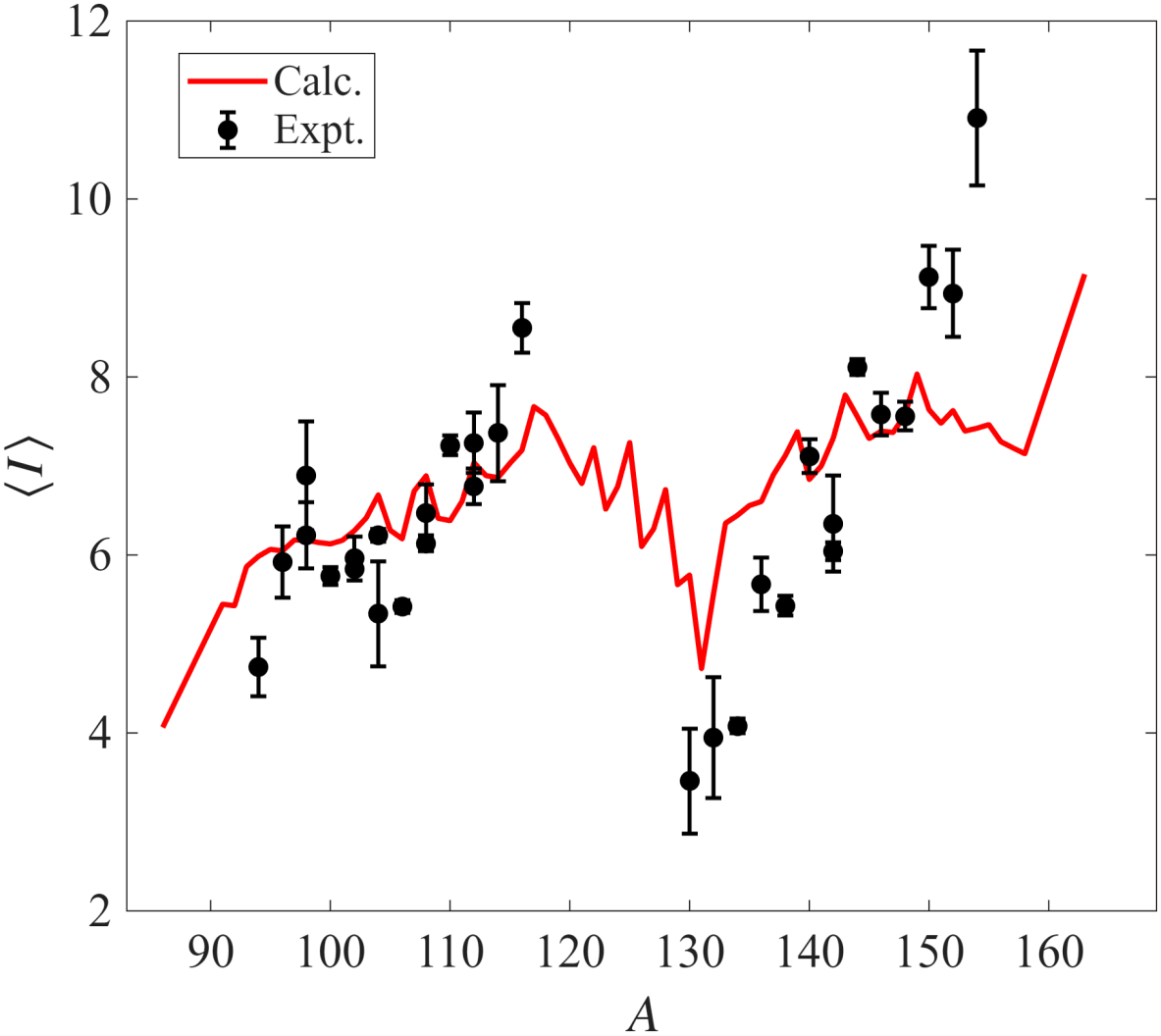
[1] G. M. Ter-Akopian et al., PRC 55, 1146 (1997).

[2] P. David et al., PLB 60, 445 (1976).

[3] N. E. Holden and M. S. Zucker, Radiation Effects 96, 289 (1986).

[4] A. S. Vorobyev et al., AIP Conf. Proc. 769, 613 (2005).

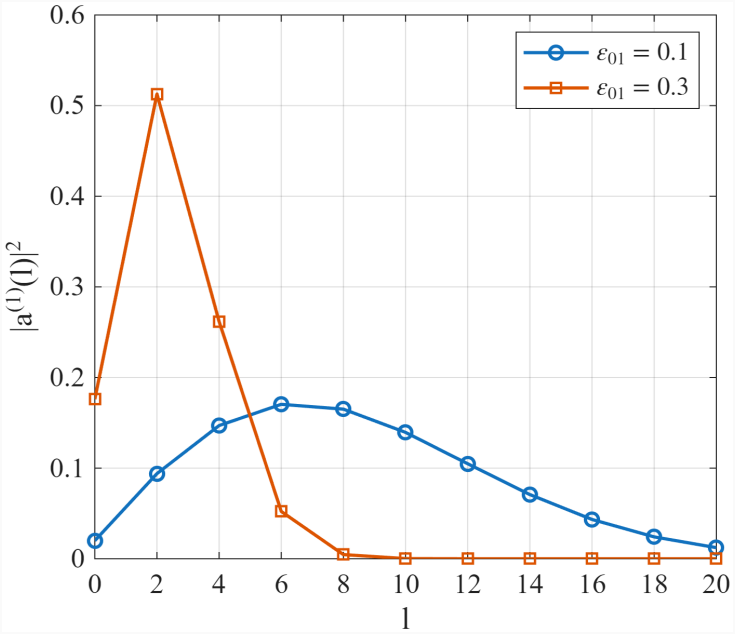
Angular momentum vs fragment mass



Expt. data from: J. N. Wilson et. al, Nature **590**, 566–570 (2021).

Role of deformation in angular momentum generation

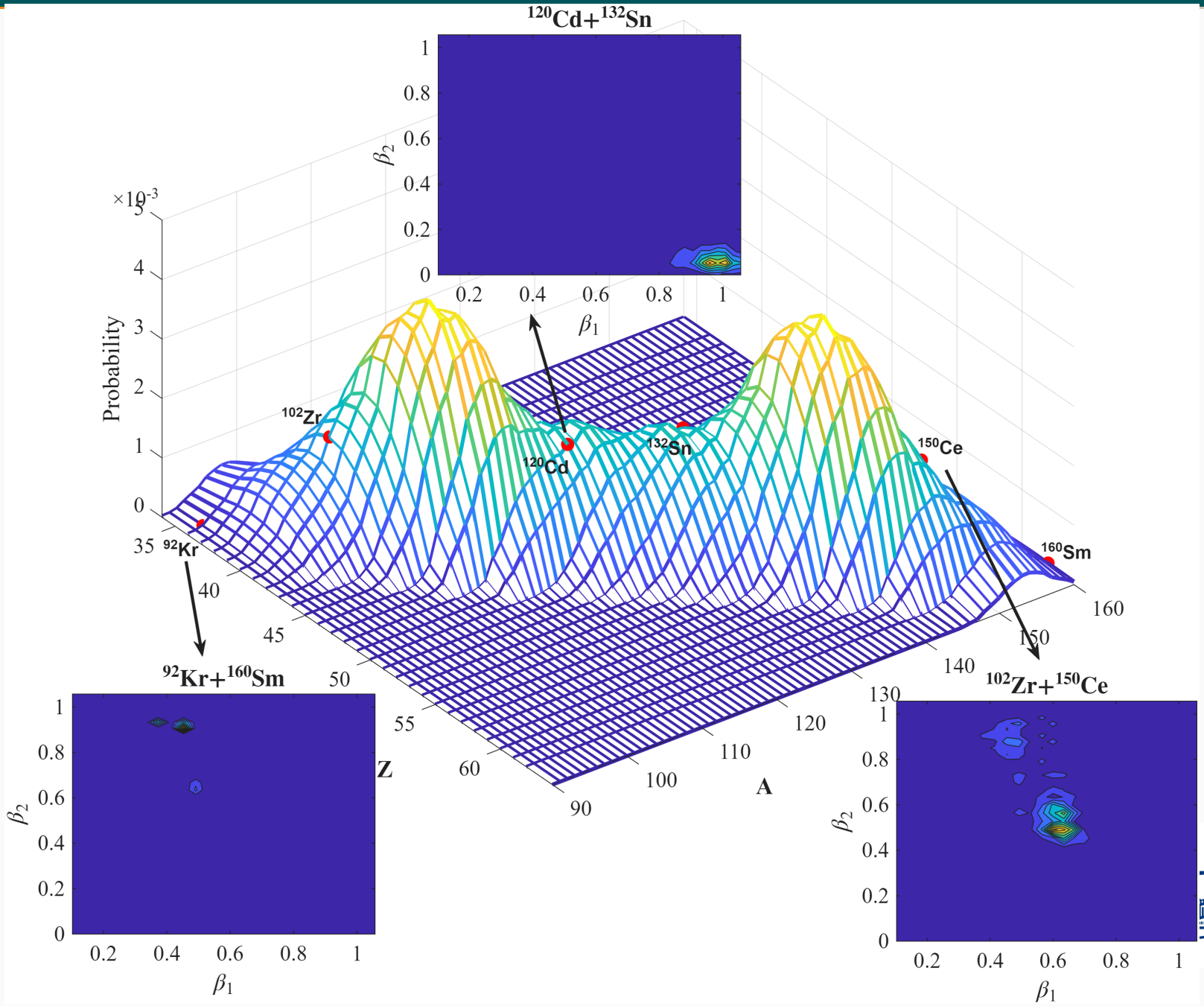
- Smaller $\varepsilon_{0i} \Longrightarrow$ more localized and more bound configuration $\Longrightarrow$ the maximum shifts toward larger angular momenta and the distribution broadens.
- Larger $\varepsilon_{0i} \Longrightarrow$ a narrower angular momentum distribution.



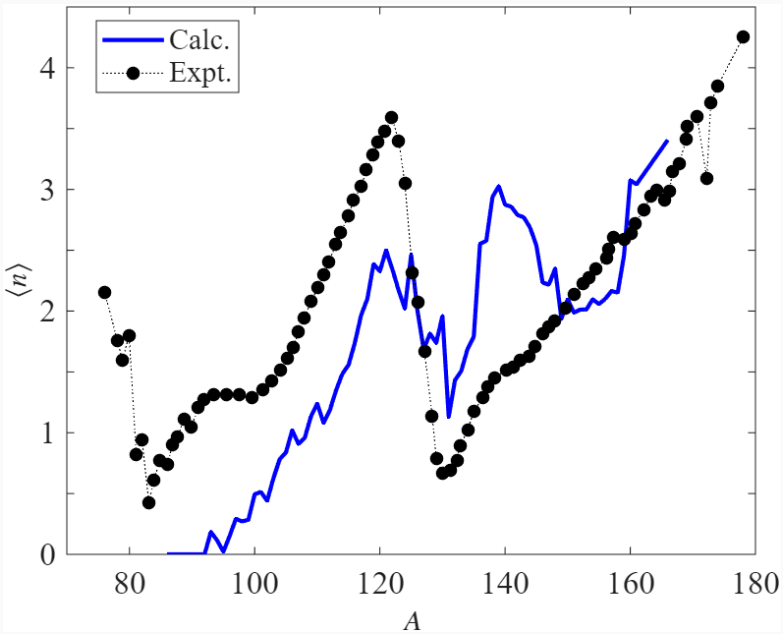
$$\Delta\varepsilon_0 \, \Delta I \sim \hbar$$

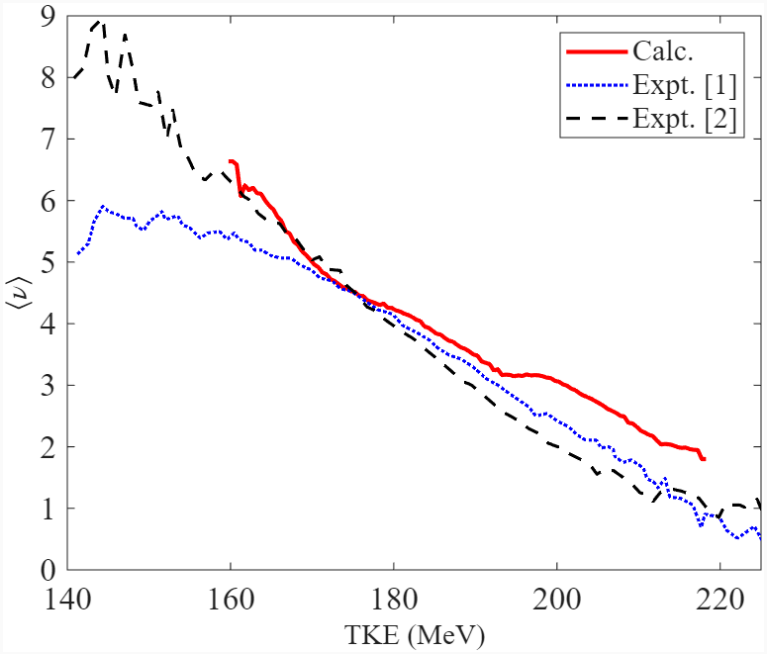
Deformation controls ε_{0i}, which in turn dictates the angular momentum distribution.

Decay-distributions of various DNS from SF of ^{252}Cf



Correlations between TKE, $< \nu >$ and A





Expt. [1]: A. Göök et al., Phys. Rev. C **90**, 064611 (2014).

Expt. [2]: S. Zeynalov et al., J. Korean Phys. Soc. 59, 1396 (2011).

Scission configurations leading to ^{144}Ba fission fragment

Expt: N. P. Giha *et al.*, Phys. Rev. C, 111 014605 (2025).

$^{144}\text{Ba} + ^{108}\text{Mo}: \quad n_{\text{Ba}} < 1$

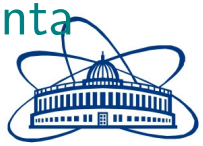
$^{145}\text{Ba} + ^{107}\text{Mo}: \quad 1 \leqslant n_{\text{Ba}} < 2,$

$^{146}\text{Ba} + ^{106}\text{Mo}: \quad 2 \leqslant n_{\text{Ba}} < 3,$

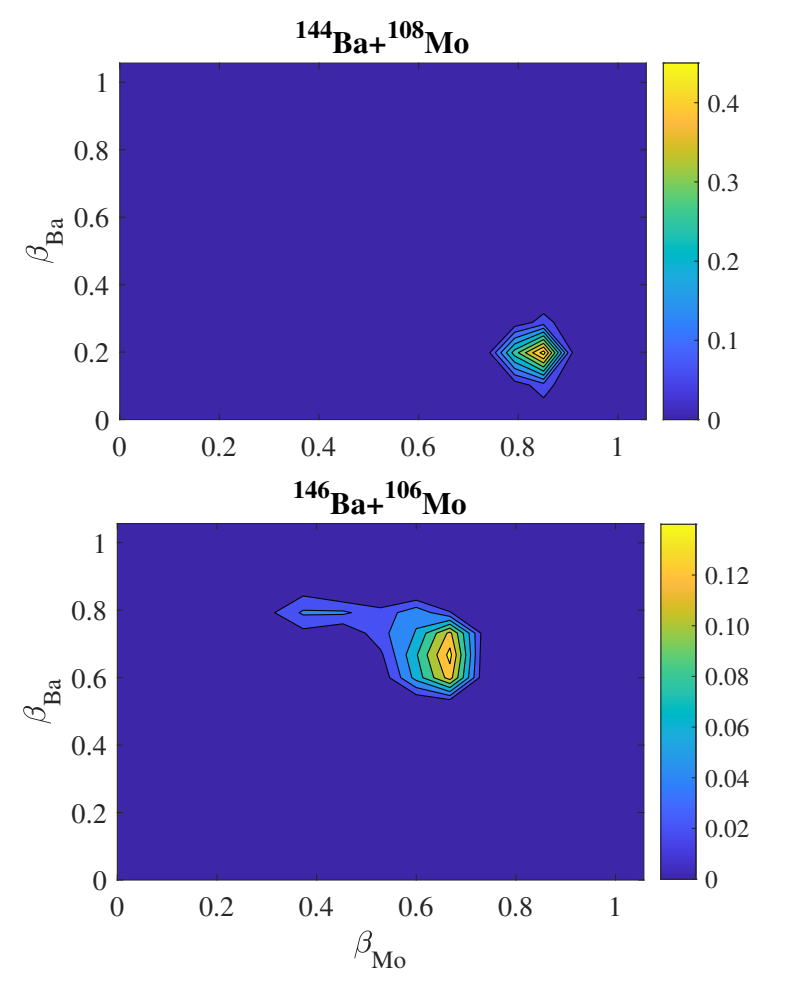
$^{147}\text{Ba} + ^{105}\text{Mo}: \quad 3 \leqslant n_{\text{Ba}} < 4$

Z_1	A_1	β_1	$< n_1 >$	Z_2	A_2	β_2	$< n_2 >$	T	Yield
42	107	0.822	2	56	145	0.453	1	0.41	0.0676
42	107	0.793	2	56	145	0.414	1	0.41	0.0581
42	107	0.822	2	56	145	0.414	1	0.40	0.0526
42	107	0.851	2	56	145	0.414	1	0.40	0.0496
42	107	0.793	2	56	145	0.453	1	0.41	0.0461
42	107	0.763	2	56	145	0.414	1	0.39	0.0384
42	107	0.700	1	56	145	0.414	1	0.37	0.0364
42	107	0.668	1	56	145	0.414	1	0.36	0.0320
42	106	0.700	1	56	146	0.491	2	0.41	0.0319
42	107	0.668	1	56	145	0.453	1	0.37	0.0302
42	107	0.7626	2	56	145	0.4530	1	0.40	0.0292
42	107	0.8507	2	56	145	0.4530	1	0.40	0.0287
42	107	0.7000	1	56	145	0.4530	1	0.38	0.0280
42	106	0.7000	1	56	146	0.5284	2	0.40	0.0256
42	106	0.6675	1	56	146	0.4912	2	0.39	0.0198
42	107	0.8220	2	56	145	0.3730	1	0.35	0.0180
						⋮			

Different deformations $\longrightarrow$ different TKE $\longrightarrow$ different angular momenta

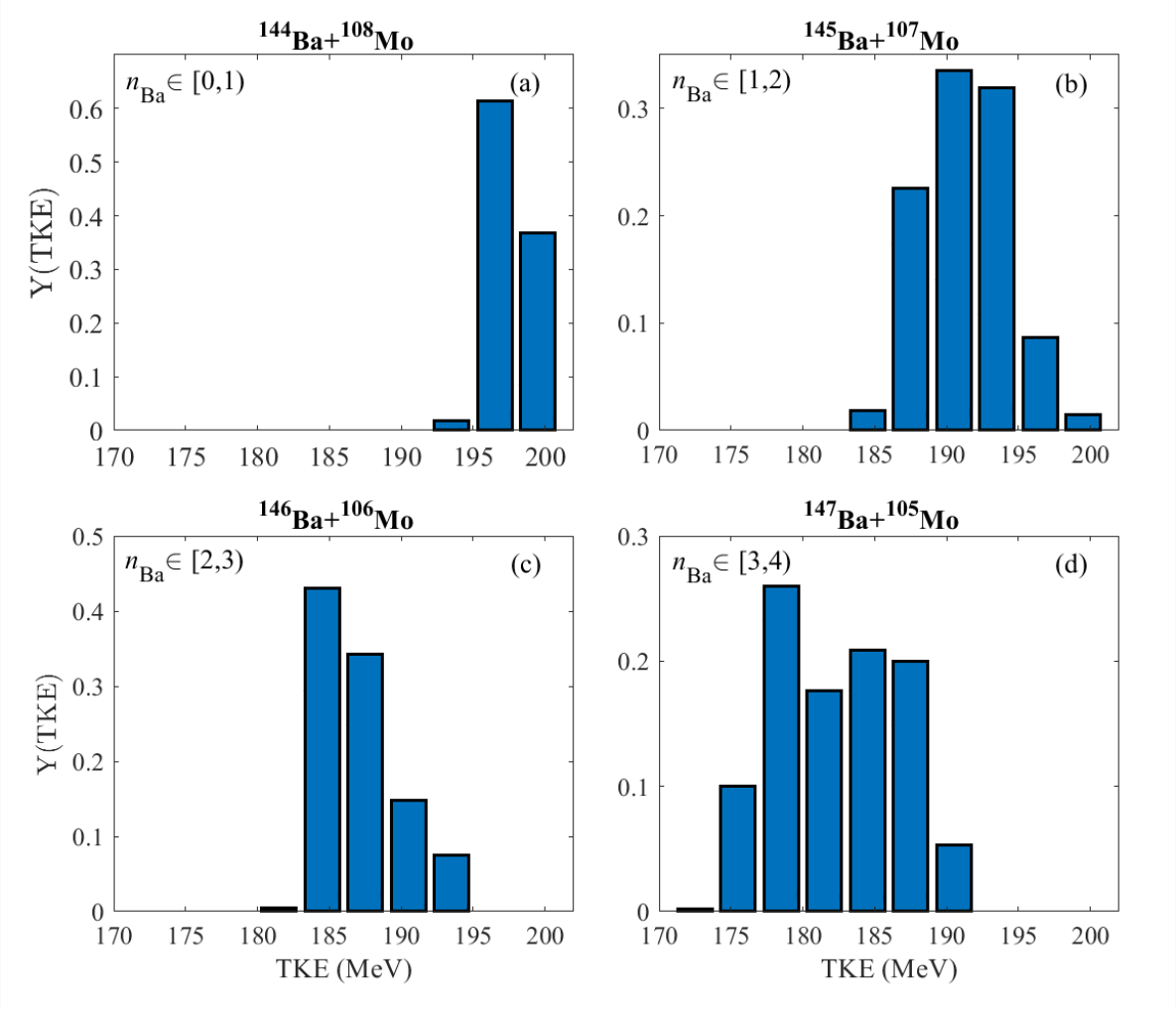


Scission configurations leading to ^{144}Ba fission fragment



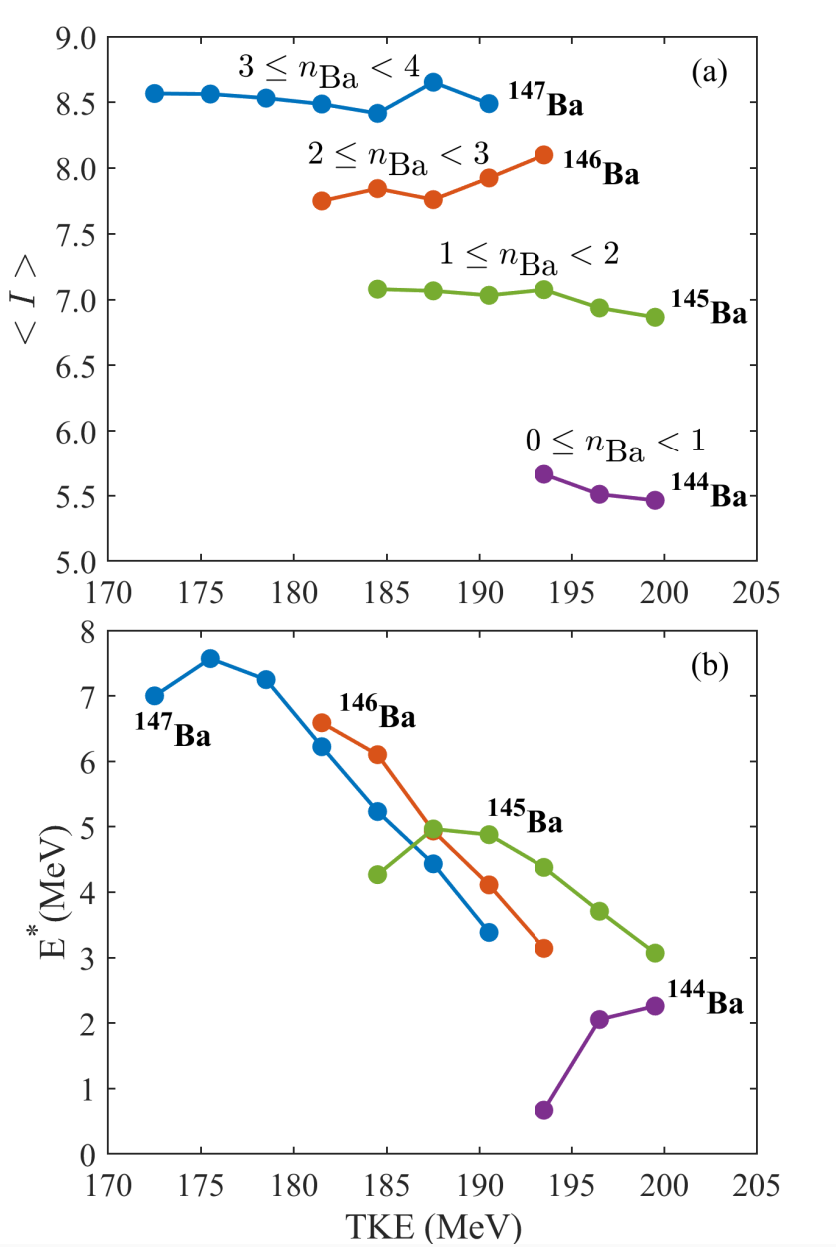
The decay probabilities of scission configurations leading to post-scission fragment ^{144}Ba as a function of the deformations β_{Mo} and β_{Ba} of the Mo and Ba fragments

TKE distribution for various scission configurations



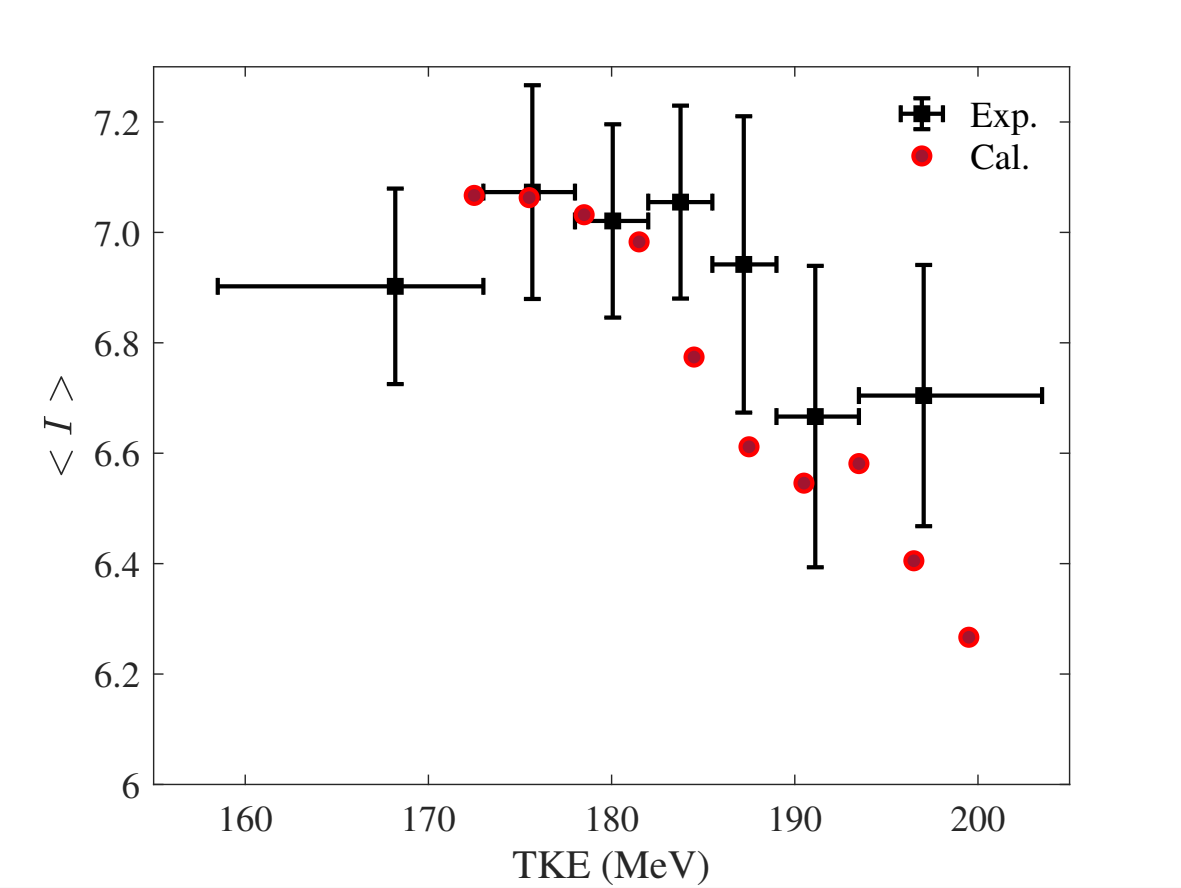
The calculated total kinetic energy distributions for the decay from various scission configurations leading to post-scission fragment ^{144}Ba. Each TKE distribution presented here is normalized to unity.

Spin vs TKE: Primary fragments



The calculated average spins and excitation energies of Ba isotopes in scission configurations leading to ^{144}Ba after n_{Ba} neutron emissions, plotted against total kinetic energy TKE.

Spin vs TKE: ^{144}Ba fragment of ^{252}Cf SF: PRC 112, 044610 (2025).



Average spins $\langle I \rangle$ of post-scission ^{144}Ba (red circles) as a function of total kinetic energy (TKE).

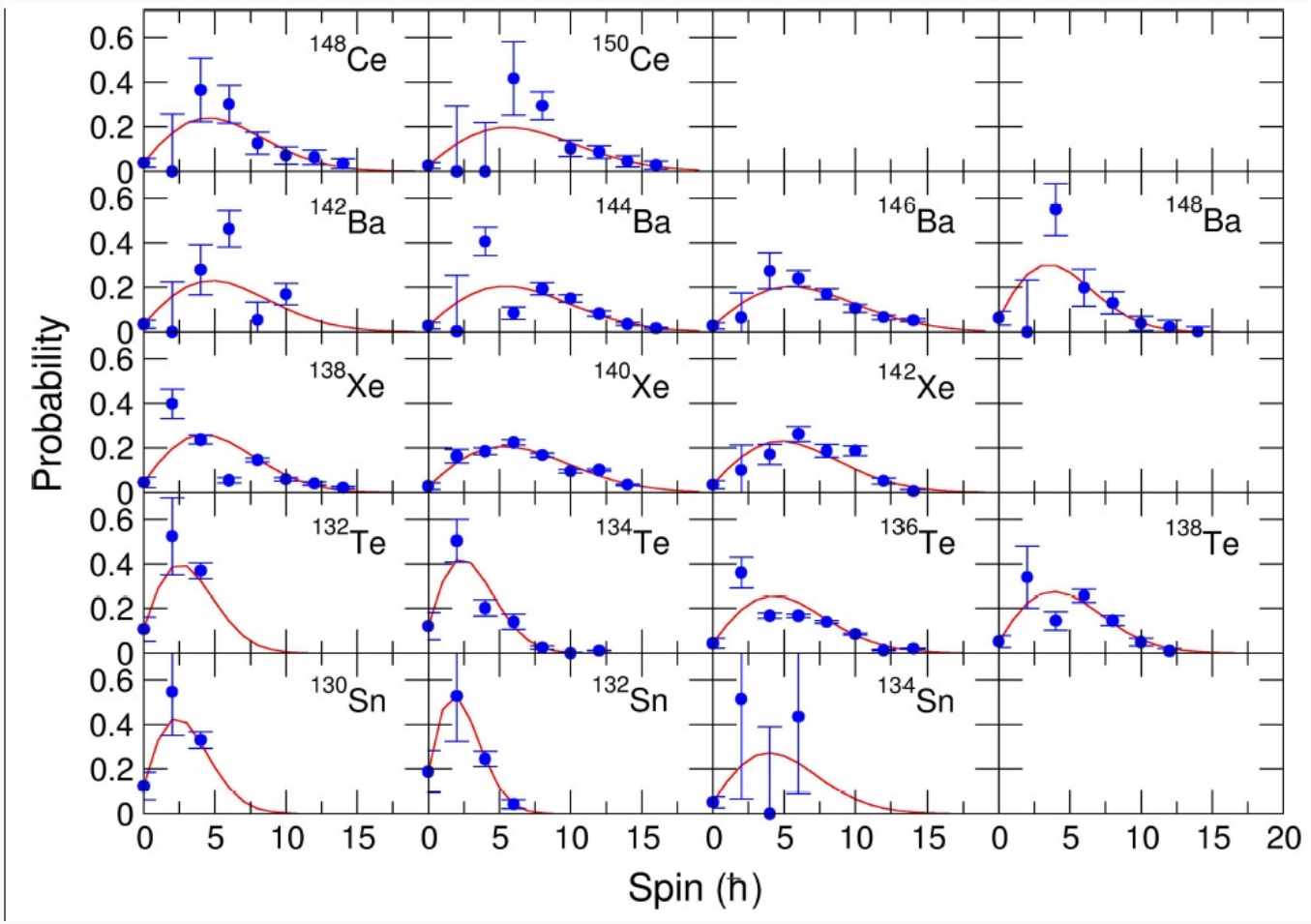
Exp. data (black squares) from N. P. Giha *et al.*, PRC **111** 014605 (2025).

Summary

- Our approach describes the evolution of a fissioning nucleus as a random walk among **DNS configurations**, successfully explaining the correlations between TKE, neutron multiplicity, and fragment masses in the SF of ^{252}Cf.
- An **analytical expression** for distribution of angular momenta of fission fragments is obtained.
- Most of energy available for neutron emission is stored as **deformation** energy while the excitation energy at scission is rather small and the excitation of higher-lying states of collective angular motions is strongly hindered.
- The **saw-tooth** behavior of $< \nu >$ and $< I >$ is explained as due to enhanced stiffness of fragments in the Sn region.

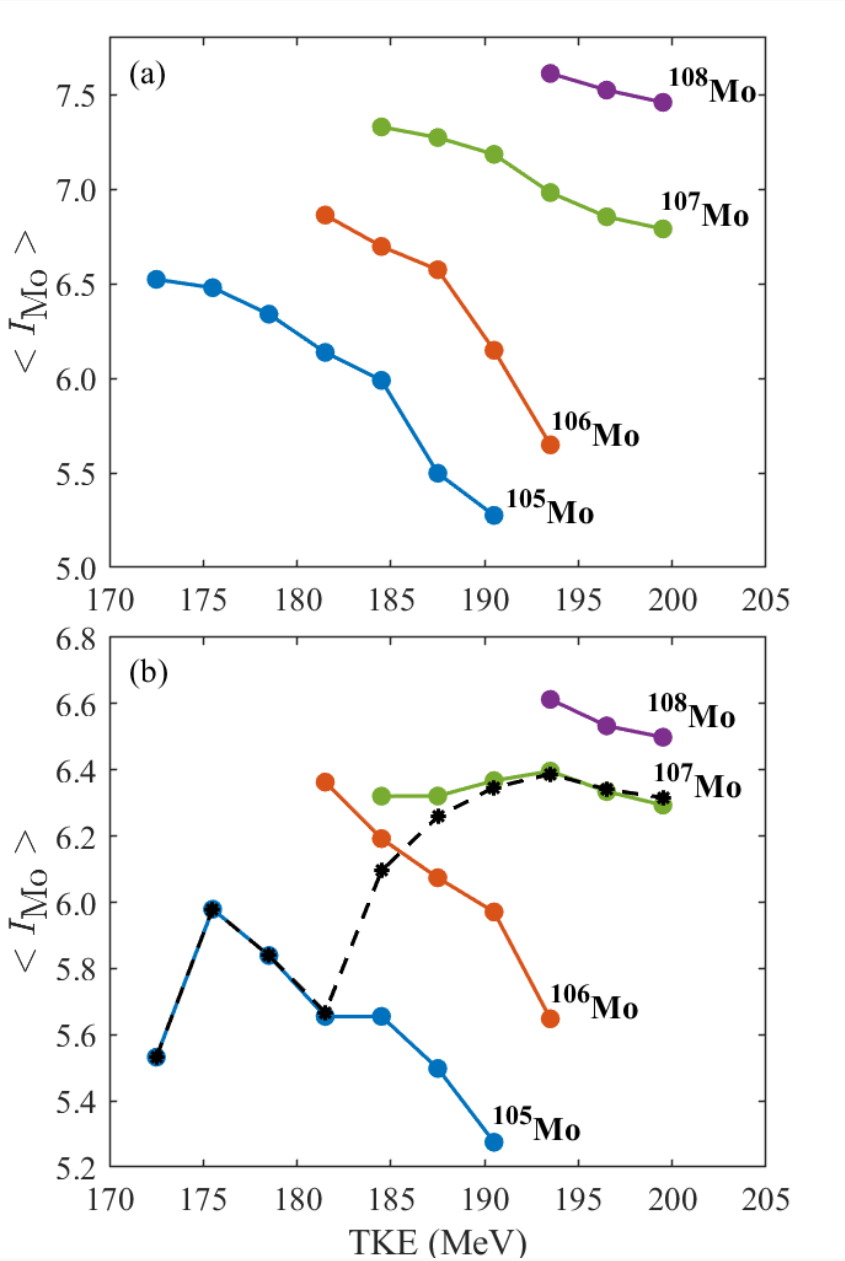
Thank You!



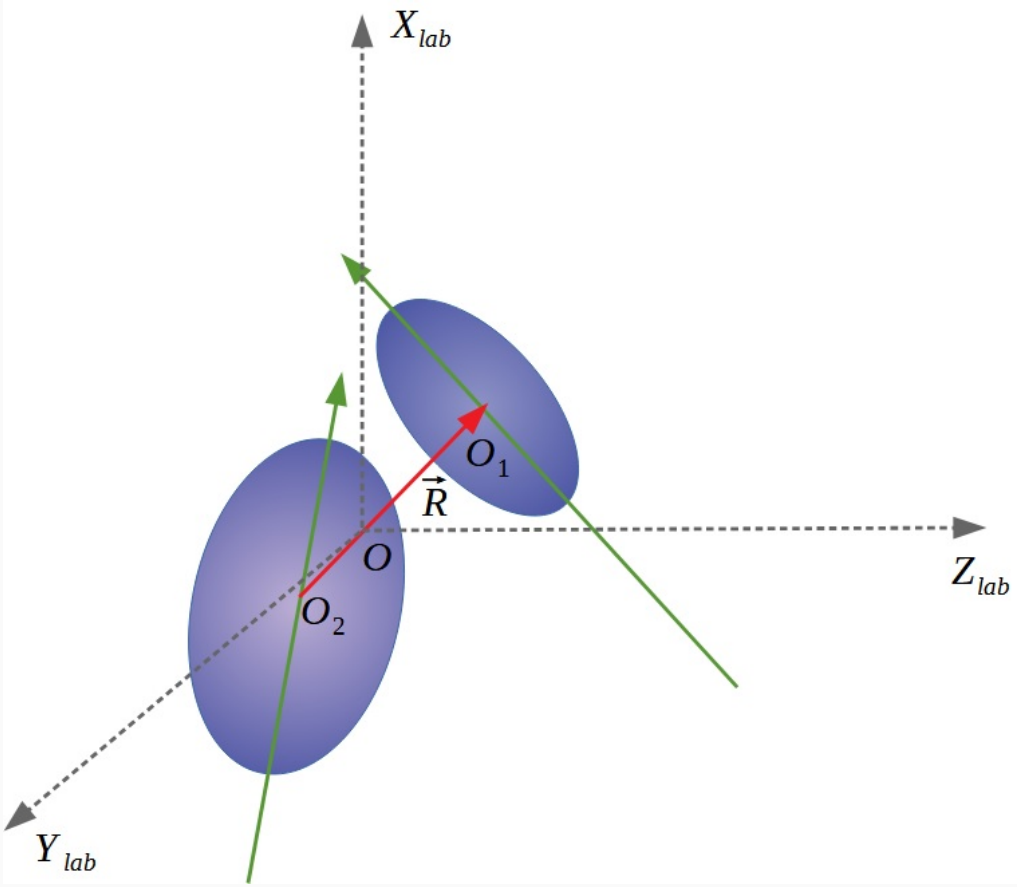


J. N. Wilson et. al, Nature **590**, 566–570 (2021).

Spin vs TKE: ^{108}Mo



Degrees of freedom



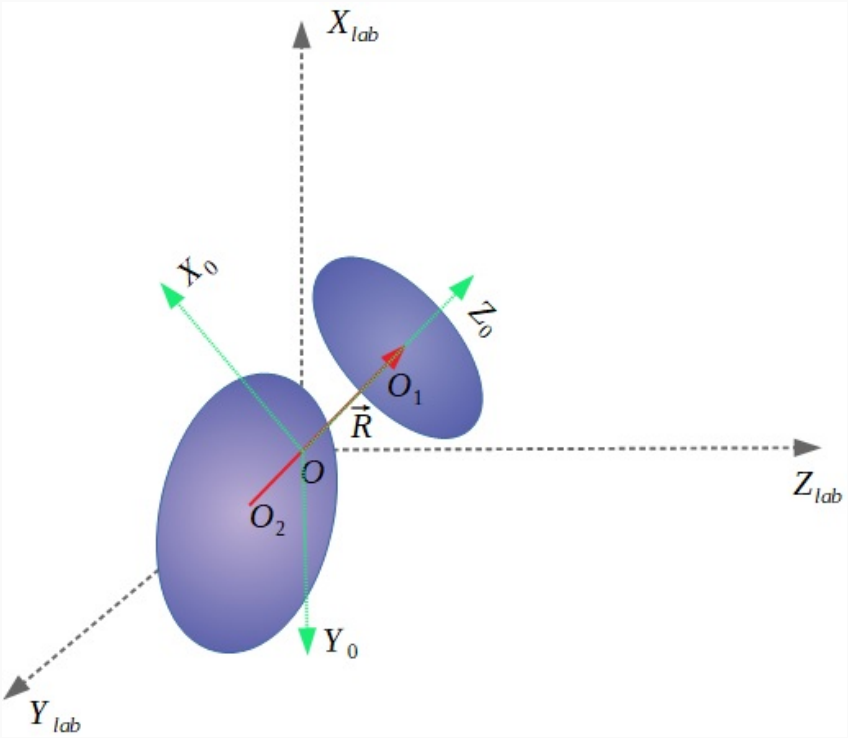
At scission, the fissile nucleus is modeled as a DNS with fragments with masses $A_{1,2}$, charges $Z_{1,2}$ in touching.

$$A_1 + A_2 = A$$

$$Z_1 + Z_2 = Z$$

The fragments are characterized by axially-symmetric quadrupole deformation parameters $\beta_{1,2}$. The vector **R** connects the centers of masses of the fragments.

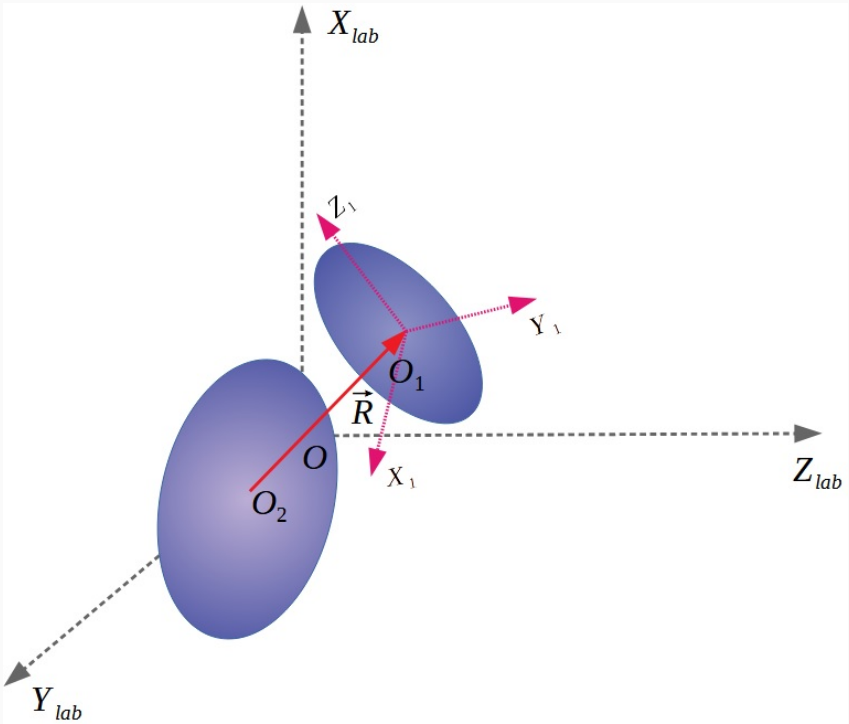
Degrees of freedom



$\Omega_0(\phi_0, \theta_0, 0)$:

Euler angles of body-fixed system with respect to lab system.

Degrees of freedom



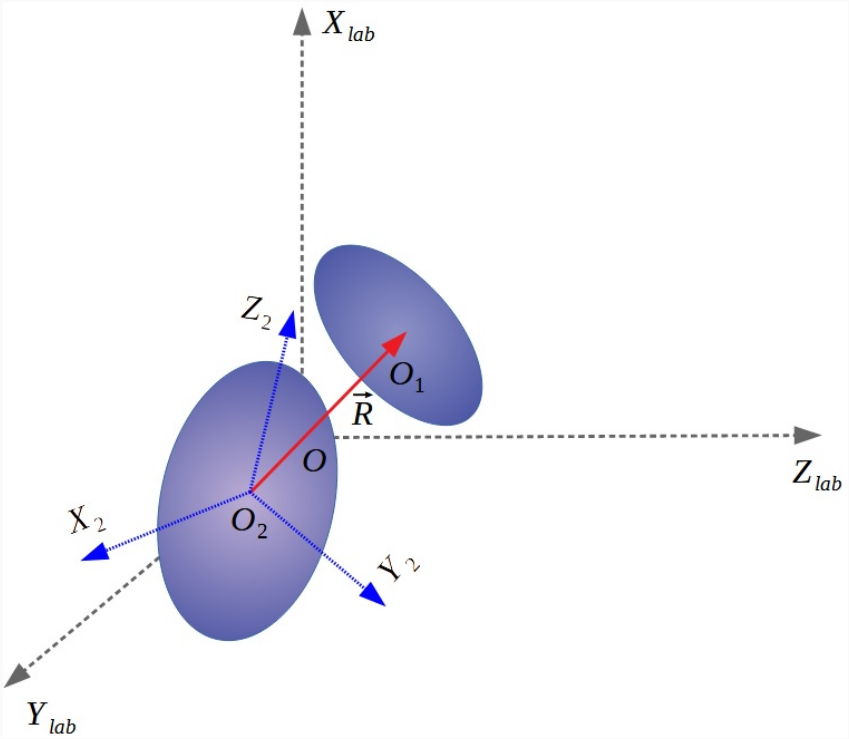
$\Omega_0(\phi_0, \theta_0, 0)$:

Euler angles of body-fixed system with respect to lab system.

$\Omega_1(\phi_1, \theta_1, 0)$:

Euler angles of intrinsic system of first fragment with respect to lab system.

Degrees of freedom



$\Omega_0(\phi_0, \theta_0, 0)$:
Euler angles of body-fixed system with respect to lab system.

$\Omega_1(\phi_1, \theta_1, 0)$:
Euler angles of intrinsic system of first fragment with respect to lab system.

$\Omega_2(\phi_2, \theta_2, 0)$:
Euler angles of intrinsic system of second fragment with respect to lab system.

Hamiltonian of angular motion in DNS: $H = T + V$

Kinetic energy:

$$T = \frac{\hbar^2 \hat{I}_0^2}{2\mu R_m^2} + \frac{\hbar^2 \hat{I}_1^2}{2\Im_1} + \frac{\hbar^2 \hat{I}_2^2}{2\Im_2}$$

Angular momentum operators:

$$\hat{I}_i^2 = -\left(\frac{1}{sin\theta_i}\frac{\partial}{\partial\theta_i} sin\theta_i \frac{\partial}{\partial\theta_i} + \frac{1}{sin^2\theta_i}\frac{\partial^2}{\partial\phi_i^2}\right), \quad \hat{I}_i^2 Y_{I_i M_i}(\Omega_i) = I_i(I_i+1) Y_{I_i M_i}(\Omega_i)$$

$\Im_{1,2}$: moments of inertia of fragments.
$\Im_R = \mu R_m^2$: moment of inertia of relative motion.

Potential energy:

$$V(R, \tilde{\Omega}_1, \tilde{\Omega}_2) = V_N(R, \tilde{\Omega}_1, \tilde{\Omega}_2) + V_{coul}(R, \tilde{\Omega}_1, \tilde{\Omega}_2), \quad \tilde{\Omega}_i = (\varepsilon_i, \gamma_i, 0)$$

$$V(\Omega_1, \Omega_2, \Omega_0) = \sum_{\lambda_0,\lambda_1,\lambda_2} V_{\lambda_0,\lambda_1,\lambda_2}(R_m) \left[Y_{\lambda_0}(\Omega_0) \times [Y_{\lambda_1}(\Omega_1) \times Y_{\lambda_2}(\Omega_2)]_{\lambda_0}\right]_{(00)}$$

Coulomb interaction

$$V_{coul} = e^2 \int \frac{\rho_1(\mathbf{r}_1)\rho_2(\mathbf{r}_2)}{|\mathbf{R}+\mathbf{r}_2-\mathbf{r}_1|} d\mathbf{r}_1 d\mathbf{r}_2.$$

$$V_{coul} = \sum_{\lambda_1\lambda_2} \sqrt{\frac{(4\pi)^2(2\lambda_1+2\lambda_2)!}{(2\lambda_1+1)!(2\lambda_2+1)!}} \frac{(-1)^{\lambda_2} Q^{(1)}_{\lambda_1}(\beta_1) Q^{(2)}_{\lambda_2}(\beta_2)}{R^{\lambda_1+\lambda_2+1}} \left[Y_{\lambda_1}(\tilde{\Omega}_1) \times Y_{\lambda_2}(\tilde{\Omega}_2) \right]_{(\lambda_1+\lambda_2,0)}$$

where

$$Q^{(i)}_{\lambda\mu}(\beta_i) = \sqrt{\frac{4\pi}{2\lambda+1}} \int \rho_i(\mathbf{r}_i) r_i^{\lambda} Y_{\lambda\mu}(\theta,\phi) d\mathbf{r}_i = Q^{(i)}_{\lambda}(\beta_i)\delta_{\mu 0} \quad (i=1,2)$$

are multipole moments of the fragments.



Nuclear interaction

Double folding potential: (G. G. Adamian *et al.*, IJMPE **5**, 191 (1996).)

$$V_N(R,\tilde{\Omega}_1,\tilde{\Omega}_2) = \int \rho_1(\mathbf{r}_1)\rho_2(\mathbf{r}_2)F(\mathbf{R}+\mathbf{r}_2-\mathbf{r}_1)\mathrm{d}\mathbf{r}_1\mathrm{d}\mathbf{r}_2,$$

with the density-dependent forces (Migdal forces):
A. B. Migdal, *Theory of finite Fermi Systems...* (Nauka, Moscow, 1982).

$$F(\mathbf{R}+\mathbf{r}_2-\mathbf{r}_1) = C_0\left(F_{in}\frac{\rho_0(\mathbf{r}_1)}{\rho_{00}} + F_{ex}\left(1-\frac{\rho_0(\mathbf{r}_1)}{\rho_{00}}\right)\right)\delta(\mathbf{R}+\mathbf{r}_2-\mathbf{r}_1),$$

$$F_{in,ex} = (f_{in,ex} + f'_{in,ex}\tau_\mathbf{1}\cdot\tau_\mathbf{2}) + (g_{in,ex} + g'_{in,ex}\tau_\mathbf{1}\cdot\tau_\mathbf{2})\sigma_\mathbf{1}\cdot\sigma_\mathbf{2}$$

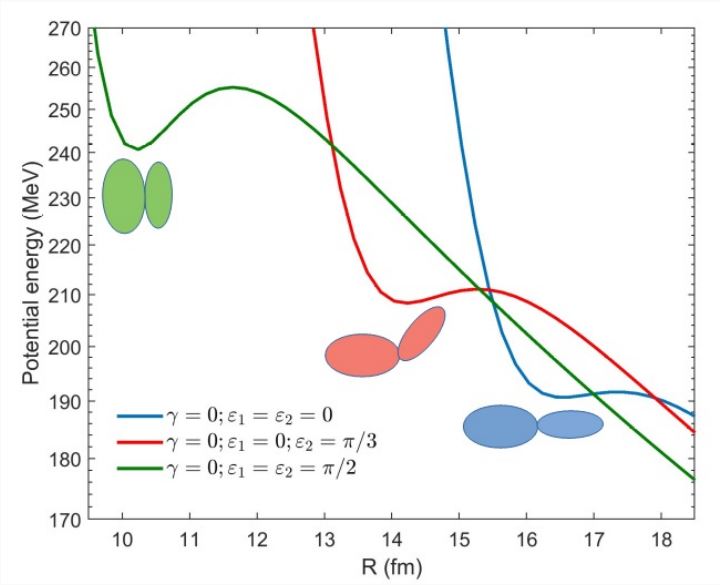
$C_0 = 300\ \mathrm{MeV\ fm}^3,\ f_{in,ex} = 0.09(-2.59),\ f'_{in,ex} = 0.42(0.54)$

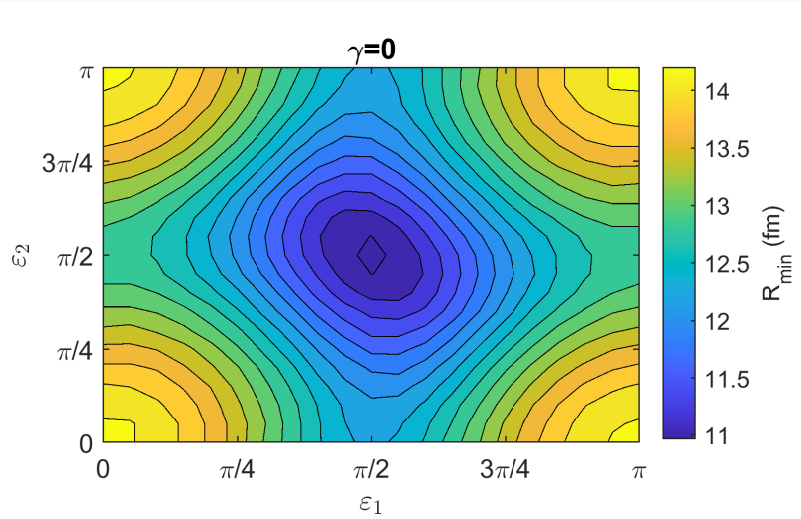
$$\rho_0(\mathbf{r}) = \rho_1(\mathbf{r}) + \rho_2(\mathbf{r}).$$

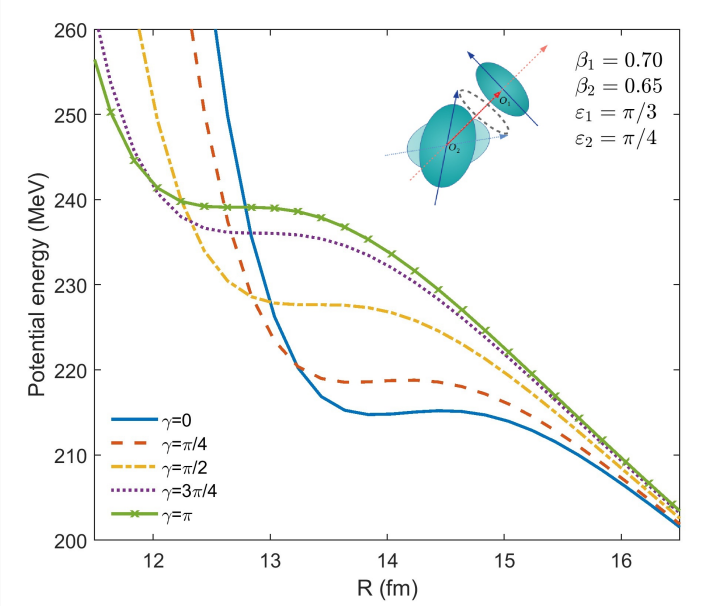
Densities are in the form of Fermi distribution.

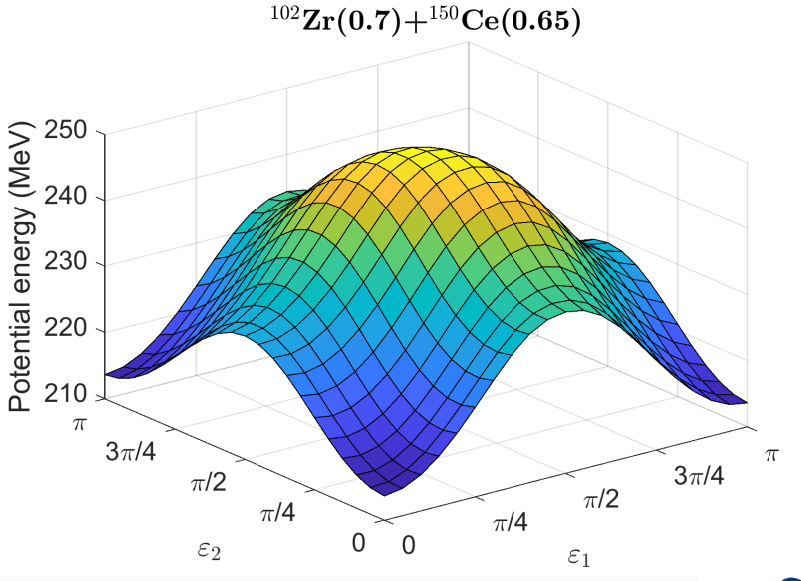


Potential energy









Basis

For a given total angular momentum I and its projection M, Hamiltonian is diagonalized on the set of tripolar spherical functions.

$$[i_0 \times [i_1 \times i_2]_{i_{12}}]_{(I,M)} \equiv \left[Y_{i_0}(\Omega_0) \times [Y_{i_1}(\Omega_1) \times Y_{i_2}(\Omega_2)]_{i_{12}}\right]_{(I,M)}$$
$$= \sum_{m_0 m_1 m_2 m_{12}} C^{IM}_{i_0 m_0, i_{12} m_{12}} C^{i_{12} m_{12}}_{i_1 m_1, i_2 m_2} Y_{i_0 m_0}(\Omega_R) Y_{i_1 m_1}(\Omega_1) Y_{i_2 m_2}(\Omega_2)$$

$$\psi^n_{IM} = \sum_{i_0 i_1 i_2 i_{12}} a^n_{i_0 i_1 i_2 i_{12}} \left[i_0 \times [i_1 \times i_2]_{i_{12}}\right]_{(IM)}$$

$\mathcal{P}(i_0 i_1 i_2) = \sum_{i_{12}} |a_{i_0 i_1 i_2 i_{12}}|^2$: Probability that angular momentum of first fragment is i_1, of second fragment is i_2, and relative angular momentum is i_0.

$$\langle I_i \rangle_n = \left[\sum_{I_0 I_1 I_2} I_i(I_i+1)\mathcal{P}(I_0 I_1 I_2)\right]^{1/2} \qquad i = 0, 1, 2$$

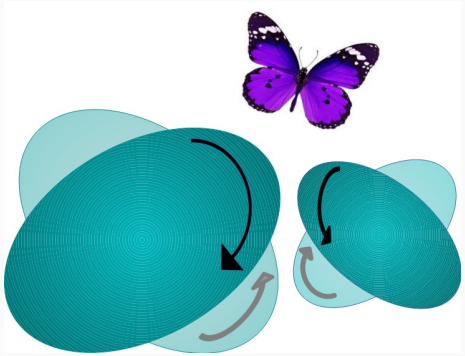


Basis for spontaneous fission

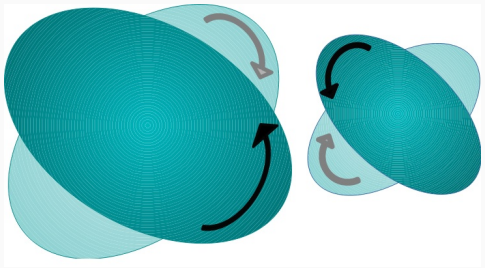
For spontaneous fission of even-even nucleus $I = M = 0 \rightarrow i_{12} \equiv i_0$

$$\psi_n = \sum_{i_0 i_1 i_2} a^n_{i_0 i_1 i_2} \left[i_0 \times [i_1 \times i_2]_{i_0} \right]_{(00)}, \quad \pi = (-1)^{l_1 + l_2 + l_0}$$

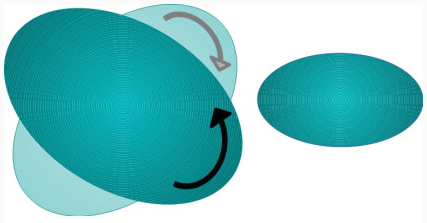
Bending mode: $[0 \times [i \times i]_0]_{(00)}$



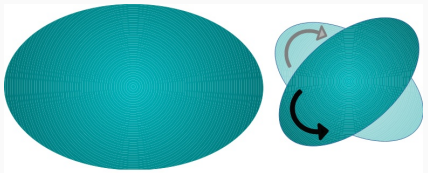
Wriggling mode:
$[2i \times [i \times i]_{2i}]_{(00)}$



Modes of independent rotation of fragments

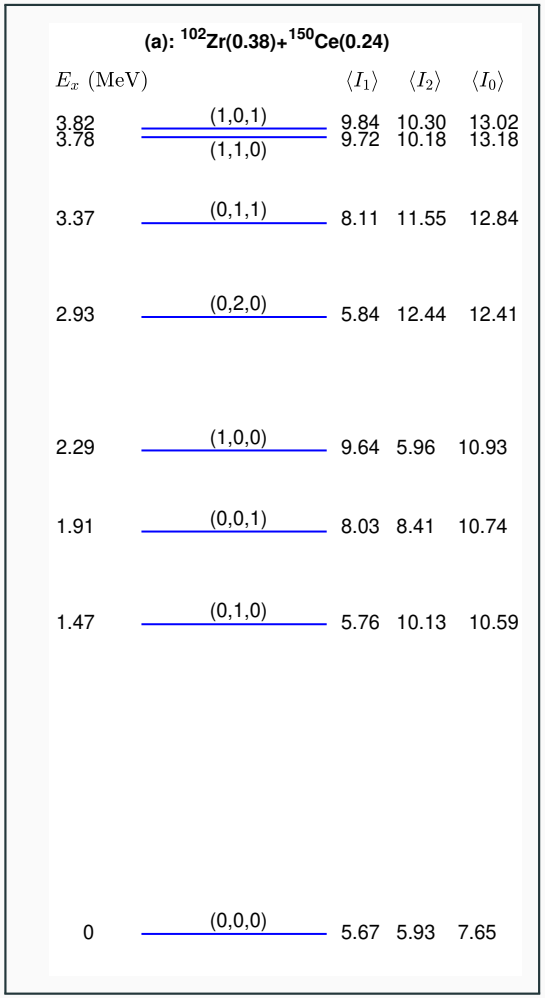


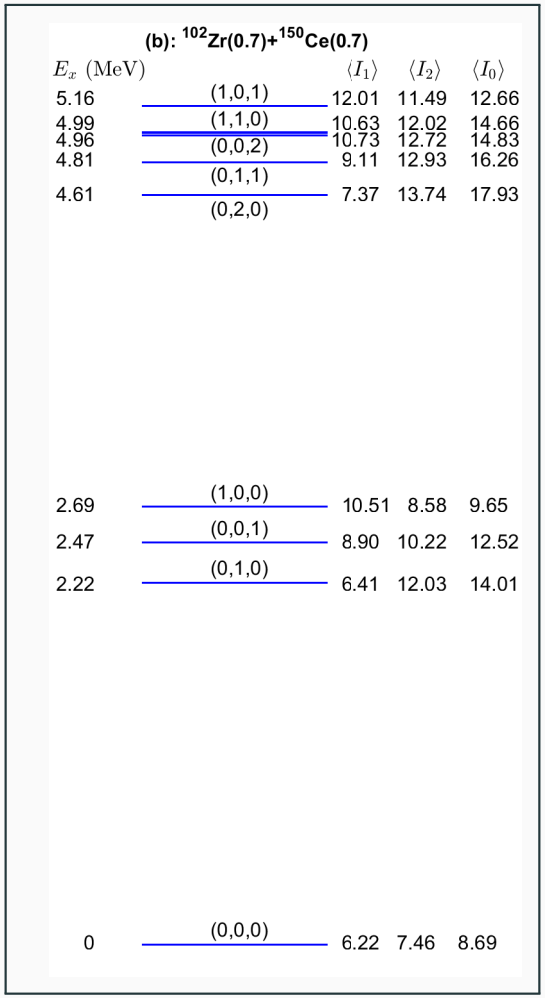
$[i \times [i \times 0]_i]_{(00)}$

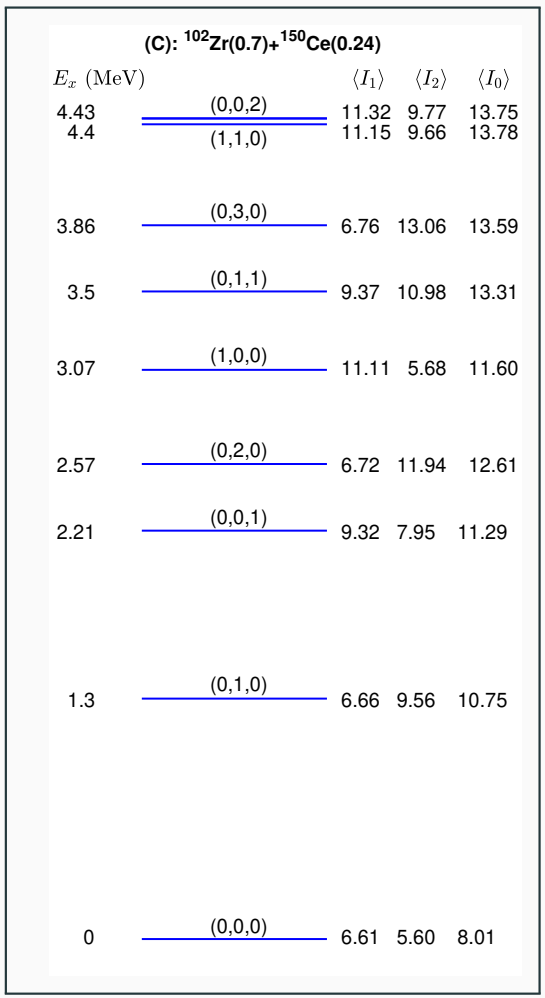


$[i \times [0 \times i]_i]_{(00)}$

Excitation spectrum of angular vibrations







$$E_{n_1,n_2,\bar{K}} = \hbar\omega_1(2n_1 + |\bar{K}| + 1) + \hbar\omega_2(2n_2 + |\bar{K}| + 1), \quad \omega_i = \sqrt{C_i/\Im_{b,i}}$$

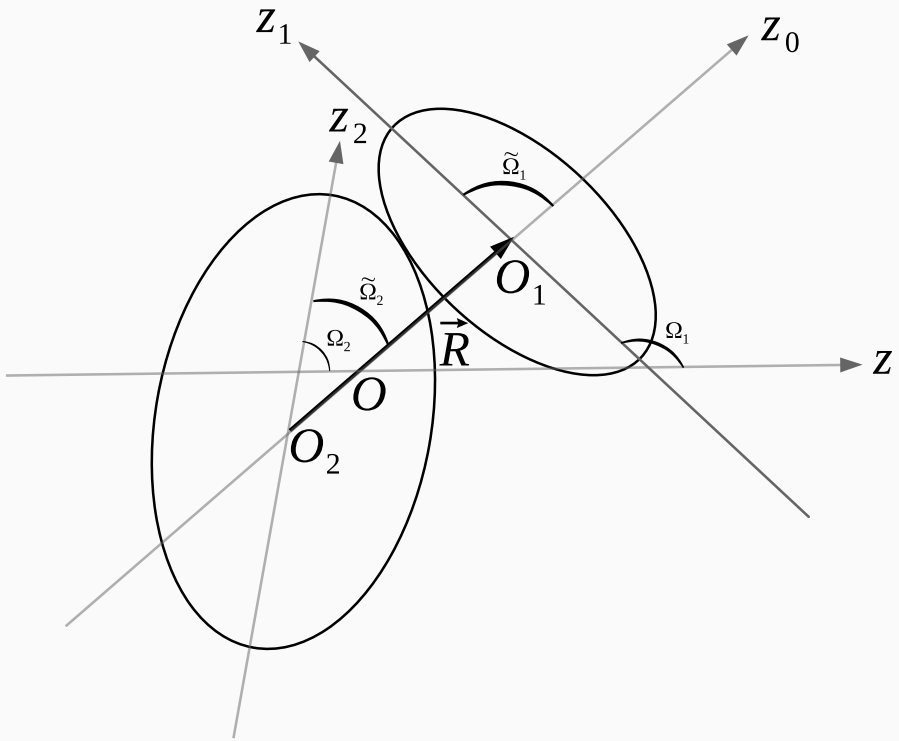
$$\Im_{b,i} = (1/\Im_0 + 1/\Im_i)^{-1} \approx \Im_i$$

T. M. Shneidman et al., Phys. Rev. C **92**, 034302 (2015).

Potential energy

Since potential energy does not depend on rotation of DNS as a whole:

$$V(R, \tilde{\Omega}_1, \tilde{\Omega}_2) = V_N(R, \tilde{\Omega}_1, \tilde{\Omega}_2) + V_{coul}(R, \tilde{\Omega}_1, \tilde{\Omega}_2)$$



$$\tilde{\Omega}_1 = (\varepsilon_1, \gamma_1, 0)$$

$$\tilde{\Omega}_2 = (\varepsilon_2, \gamma_2, 0)$$

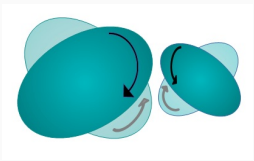
$$V(\tilde{\Omega}_1, \tilde{\Omega}_2) = \sum_{\lambda_0, \lambda_1, \lambda_2} \frac{V_{\lambda_0, \lambda_1, \lambda_2}}{\sqrt{4\pi}} \left[Y_{\lambda_1}(\tilde{\Omega}_1) \times Y_{\lambda_2}(\tilde{\Omega}_2) \right]_{(\lambda_0 0)}$$

$$\sqrt{4\pi} \left[Y_{\lambda_0}(\Omega_0) \times [Y_{\lambda_1}(\Omega_1) \times Y_{\lambda_2}(\Omega_2)]_{\lambda_0} \right]_{(00)} = \left[Y_{\lambda_1}(\tilde{\Omega}_1) \times Y_{\lambda_2}(\tilde{\Omega}_2) \right]_{(\lambda_0 0)}$$

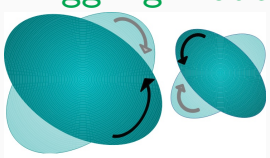
Excitation spectrum of angular vibrations

$$\begin{aligned}\Psi = &-0.101725\psi(0,2,2) - 0.108491\psi(2,0,2) - 0.106035\psi(2,2,0)\\ &+0.119896\psi(2,2,2) - 0.141349\psi(2,2,4) - 0.134025\psi(2,4,2)\\ &+0.112269\psi(2,4,4) - 0.121231\psi(2,4,6) - 0.111581\psi(2,6,4)\\ &-0.123804\psi(4,0,4) - 0.155687\psi(4,2,2) + 0.130439\psi(4,2,4)\\ &-0.140892\psi(4,2,6) - 0.114725\psi(4,4,0) + 0.123676\psi(4,4,2)\\ &-0.115071\psi(4,4,4) + 0.104944\psi(4,4,6) - 0.109322\psi(4,4,8)\\ &-0.122945\psi(4,6,2) - 0.115417\psi(6,0,6) - 0.163903\psi(6,2,4)\\ &+0.120363\psi(6,2,6) + \ldots\end{aligned}$$

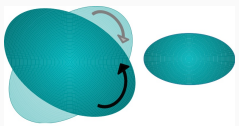
Bending mode

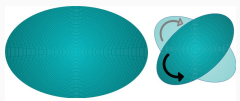


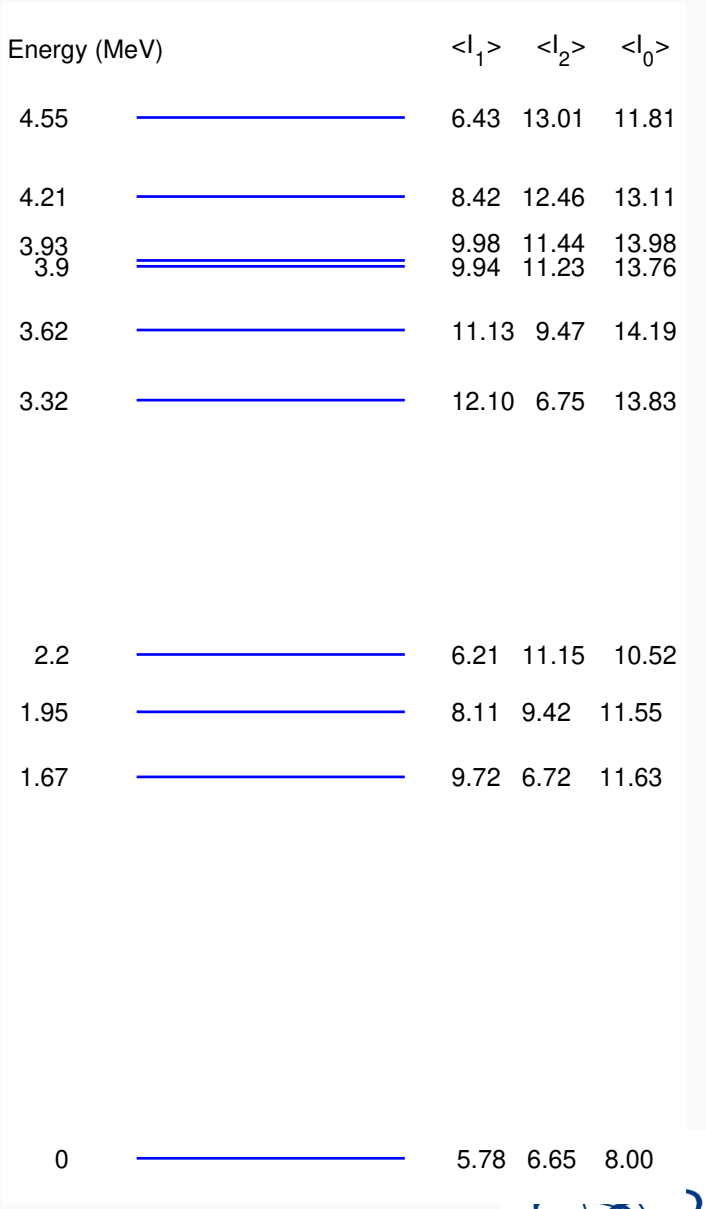
Wriggling mode

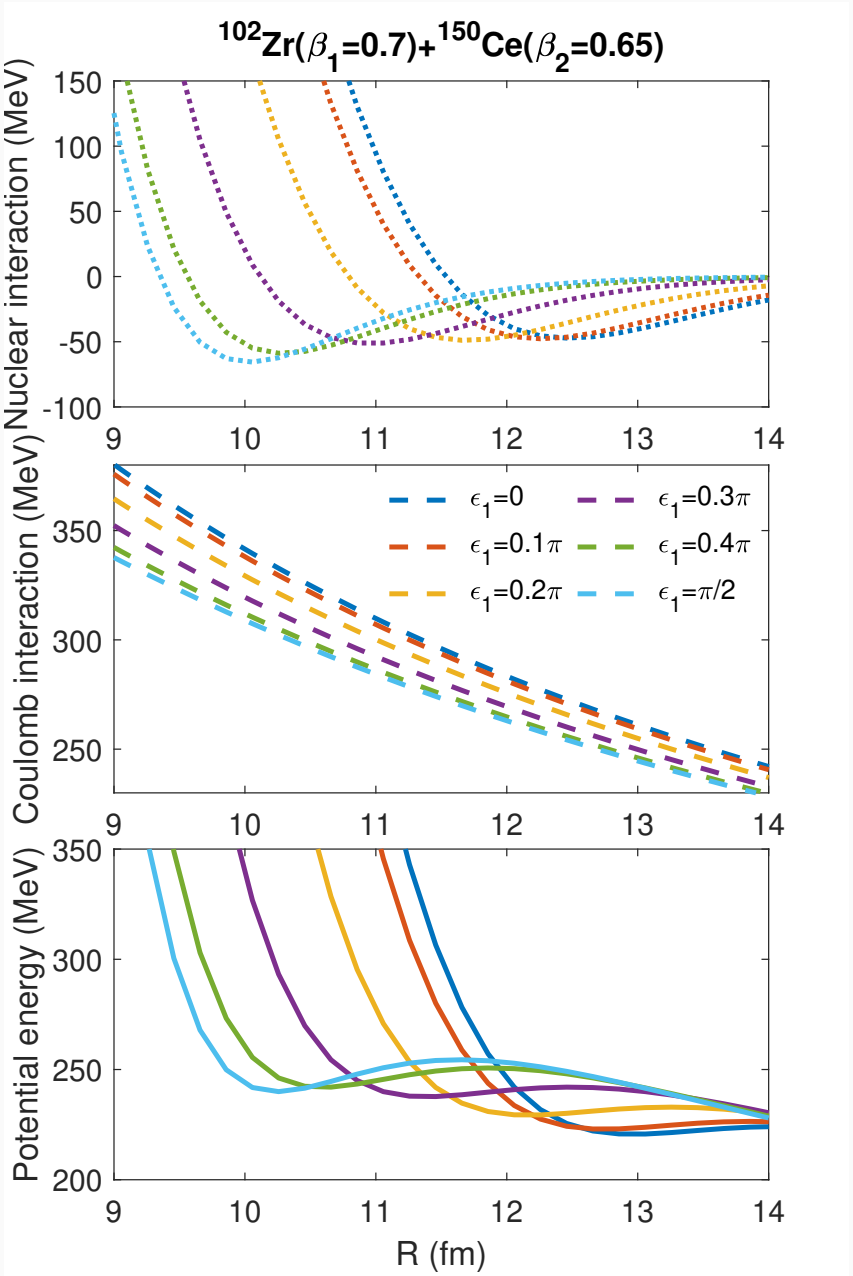


Modes of independent rotation of fragments








^{102}Zr(β_1=0.7)+^{150}Ce(β_2=0.65)
Nuclear interaction (MeV)
Coulomb interaction (MeV)
Potential energy (MeV)
R (fm)
ϵ_1=0
ϵ_1=0.1π
ϵ_1=0.2π
ϵ_1=0.3π
ϵ_1=0.4π
ϵ_1=π/2

Two independent oscillators

$$\phi^{p_i}_{n_i K_i}(\varepsilon_i, \gamma_i) = \sum_{I_i} a_{n_i I_i K_i} Y_{I_i, |K_i|}(\varepsilon_i, \gamma_i),$$

where

$$a_{n_i I_i K_i} = (-1)^{n_i} \left(\frac{(2I_i + 1)(I_i + |K_i|)!}{n_i!(n_i + |K_i|)!(I_i - |K_i|)!} \right)^{1/2}$$
$$\times \varepsilon_0^{|K_i|+1} \exp\left(-\frac{1}{2}\left(I_i + \frac{1}{2}\right)^2 \varepsilon_0^2 \right) L_n^{|K_i|}\left[(I_i + \frac{1}{2})^2 {\varepsilon_0}^2 \right].$$

Keeping in mind that

$$Y_{I_i K_i}(\pi - \varepsilon_i, \gamma_i + \pi) = (-1)^{I_i} Y_{I_i K_i}(\varepsilon_i, \gamma_i)$$

$$\phi^{+}_{n_i K_i}(\varepsilon_i, \gamma_i) = \sum_{\text{even } I_i} a_{n_i I_i K_i} Y_{I_i, |K_i|}(\varepsilon_i, \gamma_i); \quad \phi^{-}_{n_i K_i}(\varepsilon_i, \gamma_i) = \sum_{\text{odd } I_i} a_{n_i I_i K_i} Y_{I_i, |K_i|}(\varepsilon_i, \gamma_i).$$

The states with π^+ with respect to reflection contain only excitations of fragments with even angular momenta, while the π^- contain only excitations of fragments with odd angular momenta. Since we assumed the fragments are only quadrupole deformed their yrast excitation spectrum does not contain states with odd-I. Therefor, the function $\phi^{-}_{n_i K_i}(\varepsilon_i, \gamma_i)$ are identically equal to zero.



Evolution of fissioning nucleus after crossing the fission barrier

The evolution of DNS distribution in time is described using the master equation:

$$n = (Z_1, A_1, \beta_1, Z_2, A_2, \beta_2).$$

$$\frac{dP(n)}{dt} = \sum_{n' \neq n} \Lambda(n'|n)P(n') - \sum_{n' \neq n} \Lambda(n|n')P(n) - \Lambda_d(n)P(n)$$

$P(n)$ – Probability that the system is in the state n.
$P_0(n) = P(n, t = 0)$ – Probabilities of initially-formed DNS.
$\Lambda(n|n')$ – Transition rates for switching from n to n'.
$\Lambda_d(n)$ – Decay rates.

The distribution of primary fission fragments

$$P_f(n[Z_1, A_1, \beta_1, Z_2, A_2, \beta_2])$$

is obtained with Monte-Carlo technique.



Transition rates

The transition rates are expressed in terms of the microscopic transition probabilities and of the level densities of the final state.

$$\Lambda(n|n') = \lambda_{nn'}\rho(E^*_{n'}, n'), \quad \Lambda(n'|n) = \lambda_{n'n}\rho(E^*_n, n)$$

$$\lambda_{n'n} = \lambda_{nn'} = \lambda^{(i)}/\sqrt{\rho(n')\rho(n)}; \quad i = (m.a., \beta)$$

$$\Lambda_d(n) = \lambda_d \rho_{s.p.}(E^* - V_B, n)$$

$$\lambda_d = \begin{cases} 1/\sqrt{\rho_{s.p.}(n)\rho(n)}, & \text{if } (E^* > V_B) \\ 0, & \text{if } (E^* < V_B) \end{cases}$$

L.G. Moretto and J.S. Sventek, Phys. Lett. B **58**, 26 (1975).
G.G. Adamyan, A.K. Nasirov, N.V. Antonenko, R.V. Jolos , Fiz. Elem. Chastits At.Yadra **25**, 1379 (1994).



Level densities of DNS

The intrinsic level density (LD) of DNS:

$$\rho_{int}(E^*, n) = \int \rho_1(A_1, Z_1, \beta_1, \varepsilon)\rho_2(A_2, Z_2, \beta_2, E^* - \varepsilon)\mathrm{d}\varepsilon.$$

The LD of DNS fragments is calculated in superfluid formalism.

The DNS level density is obtained as a folding of intrinsic LD and the density of collective states:

$$\rho(E^*, n) = \sum_x \rho_{int}(E^* - E_x^n, n).$$

P. Decowski, et al., Nucl. Phys. A **110**, 129 (1968).

A. Bezbakh, et al., EPJA, **52**, 353 (2015).

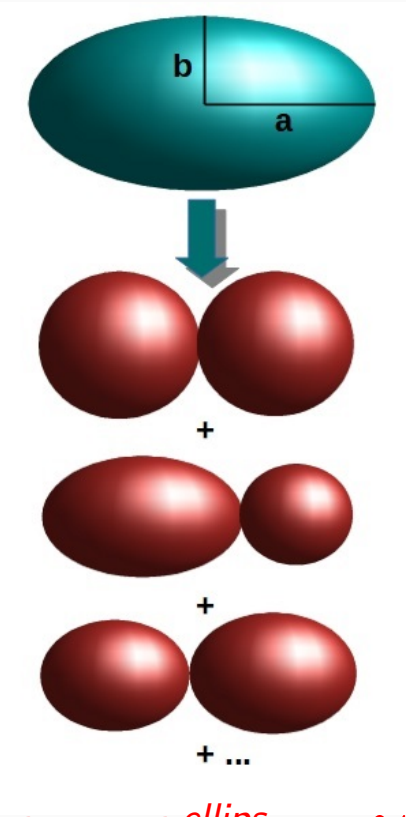
A. Rahmatinejad, et al, Phys. Rev. C, **101**, 054315 (2020).



Choice of distribution of initial states

We choose the systems whose mass quadrupole moment lies in the interval of 10% around the value of quadrupole moment of ellipsoid with axis ratio $a : b$.

$Q_2^{ellips} \sim a : b$



$Q_2 \sim Q_2^{ellips} \pm 10\%$

- **Probability of each DNS**

$$P_0(n) \sim \rho(n, E^* = U_{comp} - U_{DNS})$$

- **Quadrupole moment of DNS**

$$Q_2(n) = 2\frac{A_1 A_2}{A} R^2 + Q_2(A_1, \beta_1) + Q_2(A_2, \beta_2)$$

Various calculations show that nucleus can be presented as a DNS around $Q_2^{ellips} \sim 3 : 1$.

S. Cwiok, W. Nazarewicz et al., PLB, **322**, 304 (1994).
T. M. Shneidman et al., NPA, **671**, 119 (2000).
A. V. Afanasjev et al., Phys. Scr. **93**, 034002 (2018).